

Weak decay constant of neutral pions in a hot and magnetized quark matter

Sh. Fayazbakhsh^{a*} and N. Sadooghi^{b†}

^a*Institute for Research in Fundamental Sciences (IPM),*

School of Particles and Accelerators, P.O. Box 19395-5531, Tehran-Iran

^b*Department of Physics, Sharif University of Technology, P.O. Box 11155-9161, Tehran-Iran*

The directional weak decay constants of neutral pions are determined at finite temperature T , chemical potential μ and in the presence of a constant magnetic field B . To do this, we first derive the energy dispersion relation of neutral pions from the corresponding effective action of a two-flavor, hot and magnetized Nambu–Jona-Lasinio model. Using this dispersion relation, including nontrivial directional refraction indices, we then generalize the PCAC relation of neutral pions and derive the Goldberger-Treiman (GT) as well as the Gell–Mann-Oakes-Renner (GOR) relations consisting of directional quark-pion coupling constant $g_{qq\pi_0}^{(\mu)}$ and the weak decay constant $f_{\pi_0}^{(\mu)}$ of neutral pions.

The temperature dependence of $g_{qq\pi_0}^{(\mu)}$ and $f_{\pi_0}^{(\mu)}$ are then determined for fixed chemical potential and various constant background magnetic fields. The GT and GOR relations are also verified at finite T , μ and eB . It is shown that, because of the explicit breaking of the Lorentz invariance by the magnetic field, the directional quark-pion coupling and decay constants of neutral pions in the longitudinal and transverse directions with respect to the direction of the external magnetic field are different, i.e., $g_{qq\pi_0}^{\parallel} \neq g_{qq\pi_0}^{\perp}$ and $f_{\pi_0}^{\parallel} \neq f_{\pi_0}^{\perp}$. As it turns out, for fixed T , μ and B , $g_{qq\pi_0}^{\parallel} > g_{qq\pi_0}^{\perp}$ and $f_{\pi_0}^{\parallel} < f_{\pi_0}^{\perp}$.

PACS numbers: 12.38.-t, 11.30.Qc, 12.38.Aw, 12.39.-x

I. INTRODUCTION

Today's theory of strong interactions is quantum chromodynamics (QCD). At momentum scales of several GeV, QCD is a theory of weakly interacting quarks and gluons. At low momentum scales, however, QCD is governed by color confinement, which is accompanied by spontaneous breaking of chiral symmetry. According to the Goldstone theorem, spontaneous chiral symmetry breaking (S χ SB) implies the existence of Nambu-Goldstone (NG) bosons. For two quark flavors, up and down, the isospin triplet of neutral and charged pions is identified as the NG bosons of S χ SB. Thus, at low momentum scales, the weakly interacting pions build up the main degrees of freedom of QCD. There is strong theoretical and experimental evidence that chiral symmetry is restored at temperatures higher than 200 MeV. Crucial information on the restoration of chiral symmetry is provided by the change in the pion properties in the vicinity of the chiral transition point. Among these properties, the pions' mass, m_{π} , and weak decay constant, f_{π} , are the most important quantities, since they are deeply related to S χ SB: m_{π} and f_{π} are related to the quark bare mass and the chiral condensate via the Gell–Mann-Oakes-Renner (GOR) relation [1, 2]. To study the properties of pions, models of Nambu–Jona-Lasinio (NJL) type have been quite useful [3]. One of the basic properties of these models is that they include a gap equation that connects the chiral conden-

sate and the dynamical quark mass. This provides a mechanism for dynamical chiral symmetry breaking and the generation of quark quasiparticle masses [4]. It is known that strong magnetic fields enhance this dynamical mass generation via the phenomenon of magnetic catalysis [5, 6]. Different aspects of the effect of strong magnetic fields on the properties of quark matter were recently summarized in [7] (see, in particular, [8]).

In our previous paper [9], we have investigated the effect of external magnetic fields on the properties of neutral pions in a hot quark matter. In particular, the neutral pion mass and its directional refraction indices have been computed by making use of the effective action of a bosonized two-flavor NJL model in the presence of a constant magnetic field. We have shown that, since the presence of constant background magnetic fields breaks the Lorentz invariance, a certain anisotropy emerges in the refraction indices of neutral pions in the transverse and longitudinal directions with respect to the direction of the external magnetic field. In the present paper, we will mainly focus on the effect of external magnetic fields on the weak decay constant of neutral pions at finite temperature. We will show that this quantity exhibits the same anisotropy in the presence of constant background magnetic fields. Modifying the PCAC relation,¹ we will also prove the Goldberger-Treiman (GT)

*Electronic address: shfayazbakhsh@ipm.ir

†Electronic address: sadooghi@physics.sharif.ir

¹ The partially conserved axial vector current (PCAC) relation combined with the Feynman integral corresponding to the one-pion-to-vacuum matrix element is usually used to determine the weak decay constant of pions.

and GOR relations in the presence of external magnetic fields. The effect of a constant background magnetic field on the low energy relations of neutral pions was previously studied in [10]. Using a first order chiral perturbation theory, it was shown that f_{π^0} and m_{π^0} are shifted in such a way that the GOR relation remains valid at finite T and eB [10].

Very strong magnetic fields are supposed to be created in the early stages of noncentral heavy-ion collisions at the RHIC and LHC [11]. Depending on the collision energies and impact parameters, these magnetic fields are estimated to be of the order $eB \sim 1.5m_\pi^2$, with $m_\pi = 138$ MeV, corresponding to 0.03 GeV², and $eB \sim 15m_\pi^2$, corresponding to 0.3 GeV², respectively [12].² Although extremely short lived, the strong magnetic fields created in the heavy-ion collisions affect the properties of charged quarks in the early stage of the collision. Consequently, the properties of pions, even neutral pions, which are made of these magnetized quarks are affected by background magnetic fields. Let us emphasize that neutral pions cannot interact directly with the external magnetic fields, because of the lack of electric charge. Our method provides a possibility to study the effect of strong magnetic fields on neutral pions, at least at a theoretical level. Studying the properties of neutral pions in the final freeze-out region may provide some hints on the prehistory of their constituent quarks in the early stages of heavy-ion collisions.

The organization of this paper is as follows: In Sec. II, we will introduce the two-flavor magnetized NJL model, and, reviewing our analytical results from [9], we will derive the effective action of neutral scalar and pseudoscalar mesons, $\sigma \sim \bar{\psi}\psi$ and $\pi^a \sim \bar{\psi}i\gamma_5\tau^a\psi$, in a derivative expansion up to the second derivative.³ We will show that it includes nontrivial form factors. To study the dynamics of pions, we will mainly focus on the kinetic part of the effective action that implies a nontrivial ‘‘anisotropic’’ energy dispersion relation for neutral pions,

$$E_{\pi^0}^2 = u_{\pi^0}^{(i)2} q_i^2 + m_{\pi^0}^2. \quad (\text{I.1})$$

Here, $u_{\pi^0}^{(i)}$, $i = 1, 2, 3$ are the directional refraction indices and m_{π^0} is the mass of neutral pions. We then present our numerical results for the T dependence of $u_{\pi^0}^{(i)}$, $i = 1, 2, 3$ and m_{π^0} for fixed magnetic fields $eB = 0.03, 0.2, 0.3$ GeV² and zero chemical potential.

Comparing this case with the case of zero temperature and/or magnetic field, we arrive at following conclusions: Starting with an isospin symmetric theory at zero temperature and in a magnetic-field-free

vacuum, the refraction indices for all pions are given by

$$u_{\pi_a}^{(i)} = 1, \quad \forall i, a = 1, 2, 3. \quad (\text{I.2})$$

Thus, according to (I.1), the energy dispersion relation of neutral pions in field-free vacuum turns out to be the well-known ‘‘isotropic’’ energy-dispersion relation

$$E_{\pi_a}^2 = \mathbf{q}^2 + m_{\pi_a}^2, \quad \forall a = 1, 2, 3. \quad (\text{I.3})$$

Hence, in the chiral limit,⁴ and in field-free vacuum, massless pions propagate at the speed of light.

At finite temperature, and $eB = 0$, however, the relativistic invariance of the theory is broken by the medium, but the isospin symmetry is still preserved. In this case a single refraction index is defined for all pions by

$$u_{\pi_a}^{(1)} = u_{\pi_a}^{(2)} = u_{\pi_a}^{(3)} = u, \quad \forall a = 1, 2, 3. \quad (\text{I.4})$$

The energy dispersion relation (I.1) is therefore given by $E_{\pi_a}^2 = u^2 \mathbf{q}^2 + m_{\pi_a}^2$, for all $a = 1, 2, 3$. This relation appears e.g. in [13–15]. According to the results in [14, 15], the refraction index u , being a T -dependent quantity, is always smaller than unity (i.e. $u < 1$). Thus, as it turns out, in the chiral limit, massless pions move at a speed slower than the speed of light [16, 17].

In [9], we have studied the case $T \neq 0$ and $eB \neq 0$, and shown that the effect of the magnetic field is twofold: First, the isospin symmetry of the theory breaks down. Consequently, neutral and charged pions exhibit different properties in the presence of background magnetic fields. Second, for a magnetic field aligned in a fixed direction, a certain anisotropy appears in the transverse and longitudinal directions with respect to this fixed direction. In [9], we have only considered the case of neutral pions, and we assumed that the magnetic field is directed in the third direction. Here, the above-mentioned anisotropy is reflected in the directional refraction indices as [9]

$$u_{\pi^0}^{(1)} = u_{\pi^0}^{(2)} \neq u_{\pi^0}^{(3)}. \quad (\text{I.5})$$

Thus, the magnetized neutral pions satisfy the anisotropic energy dispersion relation (I.1). Within our truncation up to second order derivative expansion,⁵ the transverse refraction indices $u_{\pi^0}^{(1)} = u_{\pi^0}^{(2)} > 1$, and the longitudinal one $u_{\pi^0}^{(3)} = 1$, and they do not depend on temperature and/or magnetic fields [see Fig. 4(b) in Sec. II]. As concerns the chiral limit, it turns out that whereas the massless pions propagate in the

² To keep the notation as standard as possible, we use in this paper GeV² instead of (GeV)². Note that $eB = 1$ GeV² corresponds to $b \sim 1.7 \times 10^{20}$ Gauß.

³ Here, τ^a , $a = 1, 2, 3$ are Pauli matrices. Moreover, $\pi^0 \equiv \pi_3$ and $\pi^\pm \equiv \frac{1}{\sqrt{2}}(\pi_1 \mp i\pi_2)$.

⁴ The chiral limit is characterized by $m_0 \rightarrow 0$, where m_0 is the bare mass of up and down quarks. This in turn implies $m_{\pi_a} \rightarrow 0$.

⁵ The contributions arising from pion-pion interactions are not included in our computation.

direction parallel to the magnetic field with the speed of light, their velocity in the plane perpendicular to the direction of the B field is larger than 1.⁶ The natural question arising at this stage is how these results are reflected in the other properties of neutral and massive pions, in particular, in their low energy relations. In Secs. III-IV of the present paper, we have tried to answer this question by computing the “directional” weak decay constant of neutral pions using a *modified* PCAC relation, that leads naturally to *modified* GT and GOR relations.

In Sec. III, we prove the GT and GOR relations in two different cases: In Sec. III A, using the main arguments presented in [3], we will first assume that the pions satisfy the ordinary isotropic energy dispersion relation (I.3). We will then combine the ordinary PCAC relation

$$\langle 0 | J_{\mu,5}^a(0) | \pi^b(q) \rangle = f_\pi q_\mu \delta^{ab}, \quad (\text{I.6})$$

and the Feynman integral corresponding to the one-pion-to-vacuum matrix element, and then derive the ordinary GT as well as GOR relations

$$g_{qq\pi} f_\pi = m + \mathcal{O}(m_0^2), \quad (\text{I.7})$$

as well as

$$m_\pi^2 f_\pi^2 = \frac{m_0 \sigma_0}{2G} + \mathcal{O}(m_0^2). \quad (\text{I.8})$$

Here, $J_{\mu,5}^a \equiv \bar{\psi} \gamma_\mu \gamma_5 \lambda^a \psi$, with $\lambda^a = \tau^a/2$, is the axial vector current, $g_{qq\pi}$ is the quark-pion coupling constant, $m = m_0 + \sigma_0$ is the constituent quark mass, including the bare quark mass m_0 , and the chiral condensate $\sigma_0 = -2G \langle \bar{\psi} \psi \rangle$, with G being the NJL coupling constant. In Sec. III B, we will then generalize the method presented in Sec. III A to the case of pions satisfying anisotropic energy dispersion relation (I.1). To derive the modified GT and GOR relations in this case, we will appropriately modify the PCAC relation as

$$\langle 0 | J_{\mu,5}^a(0) | \pi^b(q) \rangle = f_b q_\mu u_{\pi_b}^{(\mu)2} \delta^{ab}, \quad (\text{I.9})$$

for all $\mu = 0, \dots, 3$ and $a, b = 1, 2, 3$. Here, the four-vector $u_{\pi_b}^{(\mu)} \equiv (1, u_{\pi_b}^{(i)})$, with $u_{\pi_b}^{(i)}, i = 1, 2, 3$ the directional refraction indices appearing in (I.1). In (I.9), f_b is first an unknown dimensionful proportionality factor, which will then be shown to be equal to the constituent quark mass m . Following the same method

as in Sec. III A, we will derive the modified GT and GOR relations for all $\mu = 0, \dots, 3$ and $a = 1, 2, 3$ as

$$g_{qq\pi_a}^{(\mu)} f_{\pi_a}^{(\mu)} = m + \mathcal{O}(m_0^2), \quad (\text{I.10})$$

and

$$m_{\pi_a}^2 f_{\pi_a}^{(\mu)2} = u_{\pi_a}^{(\mu)2} \frac{m_0 \sigma_0}{2G} + \mathcal{O}(m_0^2), \quad (\text{I.11})$$

which, in contrast to (I.7) and (I.8), include the “directional” quark-pion coupling $g_{qq\pi}^{(\mu)}$ and weak decay constants of neutral pions $f_{\pi_a}^{(\mu)}$, as well as the directional refraction indices $u_{\pi_a}^{(\mu)}$. Note that for $\mu = 0$ (temporal direction), the GOR relation (I.11) leads to the well-known GOR relation

$$m_{\pi_a}^2 f_{\pi_a}^{(0)2} = \frac{m_0 \sigma_0}{2G} + \mathcal{O}(m_0^2), \quad (\text{I.12})$$

arising at finite temperature and zero magnetic field [16, 17].⁷ As aforementioned, the case of a non-vanishing magnetic field can be viewed as a special case, where neutral pions satisfy the anisotropic energy dispersion relation (I.1) with directional refraction indices given in (I.5). In Sec. IV, we will explicitly determine $g_{qq\pi}^{(\mu)}$ and $f_{\pi_a}^{(\mu)}$, first analytically (see Sec. IV A) and then numerically (see Sec. IV B). As it turns out, $g_{qq\pi^0}^{(0)} = g_{qq\pi^0}^{(3)} \neq g_{qq\pi^0}^{(1)} = g_{qq\pi^0}^{(2)}$, as well as $f_{\pi^0}^{(0)} = f_{\pi^0}^{(3)} \neq f_{\pi^0}^{(1)} = f_{\pi^0}^{(2)}$. In studying the T dependence of these quantities, we arrive at $g_{qq\pi^0}^{(0)} > g_{qq\pi^0}^{(1)}$ and $f_{\pi^0}^{(0)} < f_{\pi^0}^{(1)}$. Setting $a = 3$ in the GT and GOR relations (I.10) and (I.11), we will use these relations for neutral pions to prove numerically that f_3 , appearing in (I.9), is given by the constituent quark mass m . Using the numerical data for $m_{\pi^0}^2, f_{\pi^0}^{(\mu)}, u_{\pi^0}^{(\mu)}$ and m , we will compare numerically the left- and right hand side (r.h.s.) of the relation

$$m_{\pi_a}^2 f_{\pi_a}^{(\mu)2} = u_{\pi_a}^{(\mu)2} \frac{m_0 m}{2G}, \quad (\text{I.13})$$

which, comparing to the original GOR relation (I.11), includes the contributions of $\mathcal{O}(m_0^2)$. As it turns out, this relation seems to be exact for small T and eB . A slight deviation from this relation occurs at temperature above the chiral transition temperature. In Sec. V, we will summarize our results. A number of useful relations, which are used to derive the analytical results in Sec. IV, are presented in the Appendix.

⁶ In our previous paper [9], the directional refraction indices $u_{\pi^0}^{(i)}, i = 1, 2, 3$ defined by nontrivial form factors were computed with finite bare quark mass $m_0 \neq 0$. We recalculate $u_{\pi^0}^{(i)}, i = 1, 2, 3$ by assuming that $m_0 = 0$. We get again $u_{\pi^0}^{(1)} = u_{\pi^0}^{(2)} > 1$ as well as $u_{\pi^0}^{(3)} = 1$. In this paper, since we are interested in the low energy theorems satisfied by massive pions, we do not attempt to go through the discussion of superluminal pions (for more discussions see [18]).

⁷ The GOR relation $m_\pi^2 = \frac{2m_0 \langle \bar{\psi} \psi \rangle}{(\text{Re} f_\pi^t)^2}$ in finite temperature QCD appearing in [16, 17] turns out to be equivalent to (I.11) in the NJL model.

II. THE MODEL

A. Effective action of a two-flavor magnetized NJL model in a derivative expansion

Let us start with the Lagrangian density of a two-flavor gauged NJL model

$$\mathcal{L} = \bar{\psi}(x) (i\gamma^\mu D_\mu - m_0) \psi(x) + G \{ [\bar{\psi}(x)\psi(x)]^2 + [\bar{\psi}(x)i\gamma_5\vec{\tau}\psi(x)]^2 \} - \frac{1}{4} F^{\mu\nu} F_{\mu\nu}. \quad (\text{II.1})$$

Here, $\psi_{\alpha,f}^c, \bar{\psi}_{\alpha,f}^c$ are the fermionic fields, carrying Dirac $\alpha \in (1, \dots, 4)$, flavor $f \in (1, 2) = (u, d)$ and color $c \in (1, 2, 3) = (r, g, b)$ indices. Choosing the bare quark mass $m_0 \equiv m_u = m_d$, the above Lagrangian density is invariant under $SU(2)$ isospin symmetry. The global $SU_L(2_f) \times SU_R(2_f)$ chiral and $SU(3_c)$ color symmetries are guaranteed in the chiral limit $m_0 \rightarrow 0$. Fixing the external $U(1)$ gauge field, $A_\mu^{\text{ext.}}$, appearing in the covariant derivative $D_\mu \equiv \partial_\mu + ieQ A_\mu^{\text{ext.}}$, as $A_\mu^{\text{ext.}} = (0, 0, Bx_1, 0)$, a constant magnetic field is produced, which is directed in the third direction, $\mathbf{B} = B\mathbf{e}_3$. Here, $Q = \text{diag}(2/3, -1/3)$ is the charge matrix of the up and down quarks. Using $A_\mu^{\text{ext.}}$, the electromagnetic field strength tensor $F_{\mu\nu} \equiv \partial_{[\mu} A_{\nu]}^{\text{ext.}}$ is a constant tensor, with the only nonvanishing component $F_{12} = -F_{21} = B$. Defining the auxiliary meson fields σ and $\vec{\pi}$ as

$$\begin{aligned} \sigma(x) &= -2G\bar{\psi}(x)\psi(x), \\ \vec{\pi}(x) &= -2G\bar{\psi}(x)i\gamma_5\vec{\tau}\psi(x), \end{aligned} \quad (\text{II.2})$$

where $\vec{\tau} = (\tau_1, \tau_2, \tau_3)$ are the Pauli matrices, the Lagrangian density (II.1) is equivalently given by the semibosonized Lagrangian as

$$\mathcal{L}_{sb} = \bar{\psi}(x) (i\gamma^\mu D_\mu - m_0) \psi(x) - \bar{\psi}(\sigma + i\gamma_5\vec{\tau} \cdot \vec{\pi}) \psi - \frac{(\sigma^2 + \vec{\pi}^2)}{4G} - \frac{B^2}{2}. \quad (\text{II.3})$$

The effective action corresponding to (II.3), Γ_{eff} , is then determined by integrating out the fermionic fields ψ and $\bar{\psi}$,

$$e^{i\Gamma_{\text{eff}}[\Phi(x)]} = \int \mathcal{D}\psi \mathcal{D}\bar{\psi} \exp \left(i \int d^4x \mathcal{L}_{sb} \right). \quad (\text{II.4})$$

As a functional of x -dependent meson fields

$$\Phi(x) = (\varphi_0, \varphi_1, \varphi_2, \varphi_3) \equiv (\sigma, \pi_1, \pi_2, \pi_3), \quad (\text{II.5})$$

the effective action Γ_{eff} consists of two parts, $\Gamma_{\text{eff}} = \Gamma_{\text{eff}}^{(0)} + \Gamma_{\text{eff}}^{(1)}$. The tree-level part is given by

$$\Gamma_{\text{eff}}^{(0)}[\Phi(x)] = - \int d^4x \left(\frac{\sigma^2 + \vec{\pi}^2}{4G} + \frac{B^2}{2} \right), \quad (\text{II.6})$$

and the one-loop part reads

$$\Gamma_{\text{eff}}^{(1)}[\Phi(x)] = -i \text{tr}_{\{sfcx\}} \ln(iS_Q^{-1}[\Phi(x)]). \quad (\text{II.7})$$

Here, the trace operation includes a trace over discrete degrees of freedom, spinor s , flavor f and color c , as well as an integration over the continuous coordinate x . The inverse fermion propagator appearing in (II.7) is given by

$$iS_Q^{-1}[\Phi(x)] \equiv i\gamma^\mu D_\mu - [m(x) + i\gamma_5\vec{\tau} \cdot \vec{\pi}(x)], \quad (\text{II.8})$$

with $m(x) \equiv m_0 + \sigma(x)$. In what follows, we use the method used in [9] to evaluate the effective action $\Gamma_{\text{eff}}[\Phi(x)]$ in a derivative expansion up to second order. To do this, let us assume a constant field configuration $\Phi_0 \equiv (\sigma_0, \mathbf{0})$ that breaks the $SU_L(2_f) \times SU_R(2_f)$ chiral symmetry of the original action in the chiral limit. We then expand $\Phi(x)$ around this constant configuration,

$$\Phi(x) = \Phi_0 + \bar{\Phi}(x). \quad (\text{II.9})$$

Plugging (II.9) into the effective action $\Gamma_{\text{eff}}[\Phi(x)]$, we arrive first at

$$\begin{aligned} \Gamma_{\text{eff}}[\Phi] &= \Gamma_{\text{eff}}[\Phi_0] - \frac{1}{2} \int d^d x \mathcal{M}_{ij}^2[\Phi_0] \bar{\varphi}_i(x) \bar{\varphi}_j(x) \\ &\quad + \frac{1}{2} \int d^d x \chi_{ij}^{\mu\nu}[\Phi_0] \partial_\mu \bar{\varphi}_i(x) \partial_\nu \bar{\varphi}_j(x) + \dots, \end{aligned} \quad (\text{II.10})$$

where the summation over $i, j = 0, \dots, 3$ is skipped. Here, the squared mass matrix \mathcal{M}_{ij}^2 and the kinetic matrix $\chi_{ij}^{\mu\nu}$ are given by

$$\mathcal{M}_{ij}^2[\Phi_0] \equiv - \int d^d z \frac{\delta^2 \Gamma_{\text{eff}}}{\delta \varphi_i(0) \delta \varphi_j(z)} \Big|_{\Phi_0}, \quad (\text{II.11})$$

$$\chi_{ij}^{\mu\nu}[\Phi_0] \equiv - \frac{1}{2} \int d^d z z^\mu z^\nu \frac{\delta^2 \Gamma_{\text{eff}}}{\delta \varphi_i(0) \delta \varphi_j(z)} \Big|_{\Phi_0} \quad (\text{II.12})$$

Choosing, at this stage, the kinetic matrix $\chi_{ij}^{\mu\nu}$, as in [6, 9], in the form

$$\chi_{ij}^{\mu\nu}[\Phi] = (F_1^{\mu\nu})_{ij} + 2F_2^{\mu\nu} \frac{\varphi_i \varphi_j}{\Phi^2}, \quad \forall i, j = 0, \dots, 3, \quad (\text{II.13})$$

with $\Phi^2 = \sigma^2 + \vec{\pi}^2$, and plugging (II.13) into (II.10), the kinetic part of the effective action, $\Gamma_{\text{eff}}^k[\Phi]$, will then be given by $\Gamma_{\text{eff}}^k[\Phi] = \int d^d x \mathcal{L}_k[\Phi]$, where $\mathcal{L}_k[\Phi]$ is the part of the effective Lagrangian including only two derivatives,

$$\mathcal{L}_k = \frac{1}{2} (F_1^{\mu\nu})_{ij} \partial_\mu \varphi_i \partial_\nu \varphi_j + \frac{F_2^{\mu\nu}}{\Phi^2} (\varphi_i \partial_\mu \varphi_i) (\varphi_j \partial_\nu \varphi_j). \quad (\text{II.14})$$

Here, according to (II.5), the fields $\varphi_i, i = 1, \dots, 3$ are identified by the meson fields σ and $\vec{\pi}$. Following the standard algebraic manipulations presented in [9], the effective action of the two-flavor NJL model including $\sigma, \vec{\pi}$ mesons, which is valid in a truncation of the effective action up to two derivatives, reads

$$\begin{aligned} \Gamma_{\text{eff}}[\sigma, \vec{\pi}] &= \Gamma_{\text{eff}}[\sigma_0] \\ &\quad - \frac{1}{2} \int d^d x \bar{\sigma}(x) (M_\sigma^2 + \mathcal{G}^{\mu\nu} \partial_\mu^2) \bar{\sigma}(x) \\ &\quad - \frac{1}{2} \sum_{\ell=1}^3 \int d^d x \bar{\pi}_\ell(x) (M_\pi^2 + \mathcal{F}^{\mu\nu} \partial_\mu^2)_{\ell\ell} \bar{\pi}_\ell(x). \end{aligned} \quad (\text{II.15})$$

For a constant field configuration σ_0 , $\Gamma_{\text{eff}}[\sigma_0]$ is given by $\Gamma_{\text{eff}}[\sigma_0] = -\mathcal{V}\Omega_{\text{eff}}$, where \mathcal{V} denotes the four-dimensional space-time volume and Ω_{eff} is the effective (thermodynamic) potential. In [9], the thermo-

dynamic potential of this model is derived at finite temperature T , finite chemical potential μ , and in the presence of constant magnetic field B . It reads

$$\begin{aligned} \Omega_{\text{eff}}(m; T, \mu, eB) &= \frac{\sigma_0^2}{4G} + \frac{B^2}{2} - \frac{3}{2\pi^2} \sum_{q \in \{\frac{2}{3}, -\frac{1}{3}\}} |q_f eB|^2 \left\{ \zeta'(-1, x_{q_f}) + \frac{x_{q_f}^2}{4} + \frac{x_{q_f}}{2}(1 - x_{q_f}) \ln x_{q_f} \right\} \\ &+ \frac{3}{4\pi^2} \left\{ m^4 \ln \left(\frac{\Lambda + \sqrt{\Lambda^2 + m^2}}{m} \right) - \Lambda(2\Lambda^2 + m^2)\sqrt{\Lambda^2 + m^2} \right\} \\ &- 3T \sum_{q_f \in \{\frac{2}{3}, -\frac{1}{3}\}} |q_f eB| \sum_{p=0}^{+\infty} \alpha_p \int_{-\infty}^{+\infty} \frac{dp_3}{4\pi^2} \left\{ \ln \left(1 + e^{-\beta(E_q + \mu)} \right) + \ln \left(1 + e^{-\beta(E_q - \mu)} \right) \right\}. \end{aligned} \quad (\text{II.16})$$

In a mean field approximation, the constant field configuration $\Phi_0 = (\sigma_0, \mathbf{0})$ is supposed to minimize the above thermodynamic potential Ω_{eff} . In (II.16), $m = m_0 + \sigma_0$, $x_{q_f} \equiv \frac{m^2}{2|q_f eB|}$, Λ is an appropriate ultraviolet (UV) momentum cutoff and $\beta \equiv T^{-1}$. Moreover, $\zeta'(-1, x_q) \equiv \frac{d\zeta(s, x_q)}{ds} \Big|_{s=1}$, where $\zeta(s, a) \equiv \sum_{p=0}^{\infty} (a+p)^{-s}$ is the Riemann-Hurwitz ζ -function, and $\alpha_p \equiv 2 - \delta_{p,0}$ is the spin degeneracy factor. In (II.16), E_q is the energy of charged fermions in a constant magnetic field, which is given by

$$E_q \equiv \sqrt{\bar{p}_q^2 + m^2} = \sqrt{2|q_f eB|p + p_3^2 + m^2}. \quad (\text{II.17})$$

It arises from the solution of the Dirac equation in the presence of a constant magnetic field using the Ritus eigenfunction method [19]. Here, \bar{p}_q is the Ritus four-momentum defined by

$$\bar{p}_q = (p_0, 0, -\text{sgn}(q_f eB)\sqrt{2|q_f eB|p}, p_3), \quad (\text{II.18})$$

where $p = 0, 1, 2, \dots$ labels the Landau levels. Using the standard definition (II.11), the squared mass matrices of σ and π mesons, M_σ^2 and $(M_\pi^2)_{\ell m}$, appearing in (II.15), are defined by

$$\begin{aligned} M_\sigma^2 &\equiv - \int d^4 z \frac{\delta^2 \Gamma_{\text{eff}}}{\delta \sigma(0) \delta \sigma(z)} \Big|_{(\sigma_0, \mathbf{0})}, \\ (M_\pi^2)_{\ell m} &\equiv - \int d^4 z \frac{\delta^2 \Gamma_{\text{eff}}}{\delta \pi_\ell(0) \delta \pi_m(z)} \Big|_{(\sigma_0, \mathbf{0})}, \end{aligned} \quad (\text{II.19})$$

$\forall \ell, m = 1, 2, 3$. The nontrivial form factors $\mathcal{G}^{\mu\nu}$ and $\mathcal{F}_{\ell m}^{\mu\nu}$, appearing in (II.15), are combinations of the form factors $(F_\alpha^{\mu\nu})_{ij}$, $\alpha = 1, 2$, and $i, j = 0, \dots, 3$, appearing in (II.13). They are defined by $\mathcal{G}^{\mu\nu} \equiv [(F_1^{\mu\nu})_{00} + 2F_2^{\mu\nu}]$ and $\mathcal{F}_{\ell m}^{\mu\nu} \equiv \frac{1}{2}[(F_1^{\mu\nu})_{\ell m} + (F_1^{\mu\nu})_{m\ell}]$. They can be determined from the kinetic part of the

effective action Γ_{eff}^k using

$$\begin{aligned} \mathcal{G}^{\mu\nu} &\equiv -\frac{1}{2} \int d^4 z z^\mu z^\nu \frac{\delta^2 \Gamma_{\text{eff}}^k}{\delta \sigma(0) \delta \sigma(z)} \Big|_{(\sigma_0, \mathbf{0})}, \\ \mathcal{F}_{\ell m}^{\mu\nu} &\equiv -\frac{1}{2} \int d^4 z z^\mu z^\nu \frac{\delta^2 \Gamma_{\text{eff}}^k}{\delta \pi_\ell(0) \delta \pi_m(z)} \Big|_{(\sigma_0, \mathbf{0})}, \end{aligned} \quad (\text{II.20})$$

$\forall \ell, m = 1, 2, 3$. Note that, according to our results in [9], the pion mass squared matrix $(M_\pi^2)_{\ell m}$ and the form factors $\mathcal{G}^{\mu\nu}$ and $\mathcal{F}_{\ell m}^{\mu\nu}$ have the following properties:

$$(M_\pi^2)_{\ell m} = -(M_\pi^2)_{m\ell}, \quad \text{and} \quad \mathcal{F}_{\ell m}^{\mu\nu} = -\mathcal{F}_{m\ell}^{\mu\nu}, \quad (\text{II.21})$$

$\forall \ell \neq m$. Moreover, $\forall \ell, m = 1, 2, 3$, $\mathcal{F}_{\ell m}^{\mu\nu} = \mathcal{F}_{\ell m}^{\mu\mu} g^{\mu\nu}$. The latter property is also shared by $\mathcal{G}^{\mu\nu}$.

In the present paper, as in [9], we are mainly interested in the properties of neutral σ and π^0 mesons in hot and magnetized quark matter. We therefore identify the π_3 meson with the neutral meson π^0 . To simplify the notations in the rest of this paper, we will denote $(M_\pi^2)_{33}$ from (II.19) by $M_{\pi^0}^2$ and $\mathcal{F}_{33}^{\mu\nu}$ from (II.20) by $\mathcal{F}^{\mu\nu}$. Plugging the effective action Γ_{eff} from (II.6) and (II.7) in (II.19) and (II.20), the squared mass matrices of neutral mesons, M_σ^2 and $M_{\pi^0}^2$, as well as the form factors $\mathcal{G}^{\mu\nu}$ and $\mathcal{F}^{\mu\nu}$ at zero (T, μ) and in the presence of a background B field, are given by

$$\begin{aligned} M_\sigma^2 &= \frac{1}{2G} - i \int d^4 z \text{tr}_{sf c} [S_Q(z, 0) S_Q(0, z)], \\ M_{\pi^0}^2 &= \frac{1}{2G} + i \int d^4 z \text{tr}_{sf c} [S_Q(z, 0) \tau_3 \gamma^5 S_Q(0, z) \gamma^5 \tau_3], \end{aligned} \quad (\text{II.22})$$

and

$$\begin{aligned}\mathcal{G}^{\mu\nu} &= -\frac{i}{2} \int d^4z z^\mu z^\nu \text{tr}_{sf_c} [S_Q(z, 0) S_Q(0, z)], \\ \mathcal{F}^{\mu\nu} &= \frac{i}{2} \int d^4z z^\mu z^\nu \text{tr}_{sf_c} [S_Q(z, 0) \tau_3 \gamma^5 S_Q(0, z) \gamma^5 \tau_3].\end{aligned}\quad (\text{II.23})$$

Here, $S_Q(x, y)$ is the Ritus fermion propagator [9, 20],

$$S_Q(x, y) = i \sum_{\vec{p}=0}^{\infty} \mathcal{D}\vec{p} e^{-i\vec{p}\cdot(x-y)} P_p(x_1) D_Q^{-1}(\vec{p}) P_p(y_1), \quad (\text{II.24})$$

with $\mathcal{D}\vec{p} \equiv \frac{dp_0 dp_2 dp_3}{(2\pi)^3}$, $\vec{p} = (p_0, 0, p_2, p_3)$, and \vec{p} is the Ritus momentum,

$$\vec{p} = (p_0, 0, -s_Q \sqrt{2|QeB|} p, p_3),$$

with $s_Q \equiv \text{sgn}(QeB)$.⁸ Having in mind that Q is a diagonal matrix with the entries $q_f = \{2/3, -1/3\}$, we will use $s \equiv \text{sgn}(q_f eB)$ for the elements of this 2×2 matrix s_Q . In (II.24),

$$\begin{aligned}P_p(x_1) &\equiv \frac{1}{2} [f_p^{+s}(x_1) + \Pi_p f_p^{-s}(x_1)] \\ &+ \frac{i s_Q}{2} [f_p^{+s}(x_1) - \Pi_p f_p^{-s}(x_1)] \gamma^1 \gamma^2.\end{aligned}\quad (\text{II.25})$$

Here, $\Pi_p \equiv 1 - \delta_{p,0}$ considers the spin degeneracy in the lowest Landau level with $p = 0$. Moreover, $f_p^{\pm s}(x_1)$ are defined by

$$\begin{aligned}f_p^{+s}(x_1) &\equiv \phi_p(x_1 - s_Q p_2 \ell_B^2), \quad p = 0, 1, 2, \dots, \\ f_p^{-s}(x_1) &\equiv \phi_{p-1}(x_1 - s_Q p_2 \ell_B^2), \quad p = 1, 2, 3, \dots,\end{aligned}\quad (\text{II.26})$$

where $\phi_p(x)$ is a function of Hermite polynomials $H_p(x)$ in the form

$$\phi_p(x) \equiv a_p \exp\left(-\frac{x^2}{2\ell_B^2}\right) H_p\left(\frac{x}{\ell_B}\right). \quad (\text{II.27})$$

Here, $a_p \equiv (2^p p! \sqrt{\pi} \ell_B)^{-1/2}$ is the normalization factor and $\ell_B \equiv |QeB|^{-1/2}$ is the magnetic length. In (II.24), $D_Q(\vec{p}) \equiv \gamma \cdot \vec{p}_Q - m$, with \vec{p}_Q the Ritus four-momentum from (II.18). Note that since $Q = \text{diag}(2/3, -1/3)$ is a 2×2 matrix in the flavor space, building the trace in the flavor space is equivalent to evaluating the sum over $q_f \in \{2/3, -1/3\}$.

⁸ The notation $\mathcal{D}\vec{p}$ appearing in (II.24), is used in a number of our previous papers (see e.g., [9, 21] to denote the Ritus measure of integration $\mathcal{D}\vec{p} \equiv \frac{dp_0 dp_2 dp_3}{(2\pi)^3}$. The symbol \mathcal{D} is not to be confused with \mathcal{D} used normally in the measure of the path integrals in quantum field theory, e.g., \mathcal{D} appearing in $\mathcal{D}\psi$ or $\mathcal{D}\bar{\psi}$ in (II.4).

In [9], the squared mass matrices of neutral bosons ($M_\sigma^2, M_{\pi^0}^2$) as well as the nontrivial form factors ($\mathcal{G}^{\mu\nu}, \mathcal{F}^{\mu\nu}$), appearing in (II.15), are determined numerically at finite (T, μ) and eB . To introduce T and μ , we used the standard replacements

$$p_0 = i\omega_n - \mu, \quad \text{and} \quad \int \frac{dp_0}{2\pi} \rightarrow iT \sum_n, \quad (\text{II.28})$$

where $\omega_n \equiv (2n+1)\pi T$ are the fermionic Matsubara frequencies. As it turns out, at finite temperature and zero magnetic field, the meson form factors satisfy

$$\begin{aligned}\mathcal{G}^{00} &= -\mathcal{G}^{11} = -\mathcal{G}^{22} = -\mathcal{G}^{33}, \\ \mathcal{F}^{00} &= -\mathcal{F}^{11} = -\mathcal{F}^{22} = -\mathcal{F}^{33}.\end{aligned}\quad (\text{II.29})$$

For nonvanishing magnetic fields, however, they exhibit a certain anisotropy arising from the explicit breaking of Lorentz invariance by the background magnetic field directed in the third direction,

$$\begin{aligned}\mathcal{G}^{00} &= -\mathcal{G}^{33} \neq \mathcal{G}^{11} = \mathcal{G}^{22}, \\ \mathcal{F}^{00} &= -\mathcal{F}^{33} \neq \mathcal{F}^{11} = \mathcal{F}^{22}.\end{aligned}\quad (\text{II.30})$$

B. Pole and screening masses of neutral mesons and their directional refraction indices: A review of our previous numerical results

The effective action $\Gamma_{\text{eff}}[\sigma, \vec{\pi}]$ from (II.15) can be used to determine the energy dispersion relations of neutral σ and π^0 mesons, which are generically denoted by M ,

$$E_M^2 = u_M^{(i)2} q_i^2 + m_M^2, \quad M \in \{\sigma, \pi^0\}. \quad (\text{II.31})$$

Here, $u_M^{(i)}$, $i = 1, 2, 3$ are the directional refraction indices in the spatial $i = 1, 2, 3$ directions. They are defined by

$$u_\sigma^{(i)} \equiv \left| \frac{\text{Re}\mathcal{G}^{ii}}{\text{Re}\mathcal{G}^{00}} \right|^{1/2}, \quad u_{\pi^0}^{(i)} \equiv \left| \frac{\text{Re}\mathcal{F}^{ii}}{\text{Re}\mathcal{F}^{00}} \right|^{1/2}. \quad (\text{II.32})$$

Moreover, m_M is the neutral mesons' pole mass given by

$$m_\sigma \equiv \left| \frac{\text{Re}M_\sigma^2}{\text{Re}\mathcal{G}^{00}} \right|^{1/2}, \quad m_{\pi^0} \equiv \left| \frac{\text{Re}M_{\pi^0}^2}{\text{Re}\mathcal{F}^{00}} \right|^{1/2}. \quad (\text{II.33})$$

In the above relations, the squared mass matrices of neutral mesons ($M_\sigma^2, M_{\pi^0}^2$), as well as form factors $\mathcal{G}^{\mu\nu}$ and $\mathcal{F}^{\mu\nu}$, are defined in (II.19) as well as (II.20). Combining the refraction indices (II.32) and the pole masses (II.33), the screening masses of neutral mesons are defined by

$$m_M^{(i)} = \frac{m_M}{u_M^{(i)}}, \quad \text{for } M \in \{\sigma, \pi^0\}, \quad \text{and } i = 1, 2, 3. \quad (\text{II.34})$$

In [9], we used (II.32)-(II.34) and determined the T dependence of the neutral mesons' pole and screening

masses as well as their refraction indices for vanishing and nonvanishing μ and eB . To do this, we first determined the T dependence of σ_0 , the minima of the thermodynamic potential Ω_{eff} from (II.16). In Fig. 1, the T dependence of the constituent quark mass $m = m_0 + \sigma_0$ is plotted for fixed $\mu = 0$ MeV and $eB = 0, 0.2, 0.5$ GeV². We observe that, for a fixed temperature, the constituent quark mass increases with increasing eB . Moreover, it turns out that the transition from the broken chiral symmetry phase, with $m \neq 0$, to the normal phase, with $m \simeq m_0 \approx 0$, is a smooth crossover, and for stronger magnetic fields the transition to the normal phase occurs at higher temperatures. All these effects are related to the phenomenon of magnetic catalysis [5, 6], according to which the constant magnetic field enhances the production of the chiral condensate $\sigma_0 \sim \langle \bar{\psi}\psi \rangle$, and therefore catalyzes the dynamical chiral symmetry breaking.

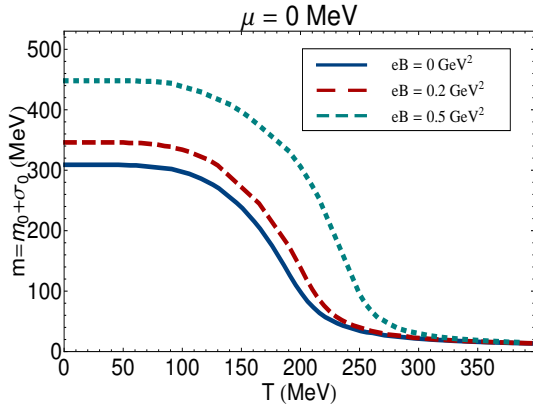


FIG. 1: The T dependence of constituent quark mass $m = m_0 + \sigma_0$ for fixed $eB = 0, 0.2, 0.5$ GeV² and fixed $\mu = 0$. Here, $m_0 \simeq 5$ MeV is the bare quark mass and σ_0 is the chiral condensate.

To determine m_σ and m_{π^0} , we further developed in [9] the necessary technique to analytically evaluate the integrals (II.22) and (II.23) up to an integration over the p_3 momentum and a summation over Landau levels and eventually performed them numerically. In Fig. 2, the T dependence of m_σ and m_{π_ℓ} , $\ell = 1, 2, 3$ is plotted for vanishing μ and eB . The free parameters of the theory, m_0, Λ and G , are chosen so that they reproduce the pion mass $m_\pi = 137.7$ MeV and $m_\sigma \simeq 824.3$ MeV, for vanishing (T, μ) and eB (see [9] and Sec. IV for more details). As it turns out, for $eB = 0$, the pion masses are degenerate, i.e., $m_{\pi_1} = m_{\pi_2} = m_{\pi_3}$. In the chirally broken phase, the temperature dependence of pions, m_{π_ℓ} , is very weak. This is because, in this phase, the pions play the role of pseudo-Goldstone modes. In the symmetry restored phase, however, pions are no longer bound states but only $q\bar{q}$ resonances [22]. In other words, they are expected to decay into (free) quarks and antiquarks.

This can only happen when m_π increases with the temperature so that $m_\pi \simeq 2m$ (see below for the definition of Mott temperature at which $m_\pi = 2m$). This is why, for temperatures larger than the crossover temperature, m_π increases with increasing T .⁹ For nonvanishing eB , as it turns out, the pion masses are not degenerate anymore. We have $m_{\pi^0} \neq m_{\pi^+} = m_{\pi^-}$. Here, the global $SU(2_f)$ symmetry breaks to a global $U(1)$ symmetry, where up and down quarks, because of their opposite electric charges, rotate with opposite angles. Thus, in the $U(1)$ symmetry broken phase and in the chiral limit, whereas charged pions become massive, the neutral pion is the only possible massless Goldstone mode [23]. As we have shown in [9], for $eB \neq 0$, the T dependence of the neutral pion mass exhibits the same behavior as $m_{\pi^0}(T)$ for $eB = 0$ (see also Figs. 2 and 3).

As concerns the σ -meson mass, in the symmetry broken phase, m_σ is large ($m_\sigma^2 = 4m^2 + m_\pi^2$ for $eB = 0$) and drops when approaching the crossover temperature [22]. In the crossover region, the σ meson dissociates into two pions (see below). For $eB = 0$, a possible explanation for this effect is provided in [24]. Here, it is shown that the σ dissociation in the crossover region is due to the occurrence of an s -channel pole in the scattering amplitude of the $\pi + \pi \rightarrow \pi + \pi$ scattering, in a process where a σ meson is coupled to the external pions via quark triangles (see e.g., [22, 24] for more details). For $eB \neq 0$, according to our results, the T dependence of the σ -meson mass is the same as $m_\sigma(T)$ for $eB = 0$ [see Fig. 3(a) and, in particular, Fig. 9(a)-(c) in [9] for more details]. Whether this behavior for $eB \neq 0$ is also related to the appearance of a certain pole in the $\pi\pi$ -scattering amplitude is an open question, which shall be investigated in the future. In the chirally restored phase m_σ and m_{π^0} , become degenerate and increase with increasing T . These results are in agreement with the results for $eB = 0$ and $T \neq 0$ recently presented in [22], where a possible definition of the crossover temperature is also provided. The latter is given by two characteristic temperatures, the σ -dissociation temperature $T_{\text{diss.}}$, defined by

$$m_\sigma(T_{\text{diss.}}) = 2m_\pi(T_{\text{diss.}}), \quad (\text{II.35})$$

and the Mott temperature T_{Mott} , defined by

$$m_\pi(T_{\text{Mott}}) = 2m(T_{\text{Mott}}). \quad (\text{II.36})$$

These temperatures were originally introduced in [24]. According to [22, 24], for $T < T_{\text{diss.}}$, the σ meson can decay into two pions, and for $T > T_{\text{Mott}}$, the pion decays into a constituent quark and antiquark; i.e., it is no longer a bound state [22]. In the chiral limit, both

⁹ In the present paper, as in [9], we mainly focus on the masses of neutral σ and π^0 mesons. The (T, μ, eB) dependence of m_{π^0} is studied in detail in [9].

temperatures are equal to the critical temperature of the chiral phase transition T_c . In Table I, we have listed $T_{\text{diss.}}$ as well as T_{Mott} for $eB = 0, 0.03, 0.2, 0.3, 0.5 \text{ GeV}^2$ and for our set of parameters.

eB in GeV^2	$T_{\text{diss.}}$ in MeV	T_{Mott} in MeV
0	175	190
0.03	175	190
0.2	193	205
0.3	206	210
0.5	250	255

TABLE I: The σ dissociation and Mott temperatures, $T_{\text{diss.}}$ and T_{Mott} , defined in (II.35) and (II.36), for vanishing and nonvanishing eB and for our set of parameters, $m_0 = 0.005 \text{ GeV}$, $\Lambda = 0.6643 \text{ GeV}$ and $G = 4.668 \text{ GeV}^{-2}$.

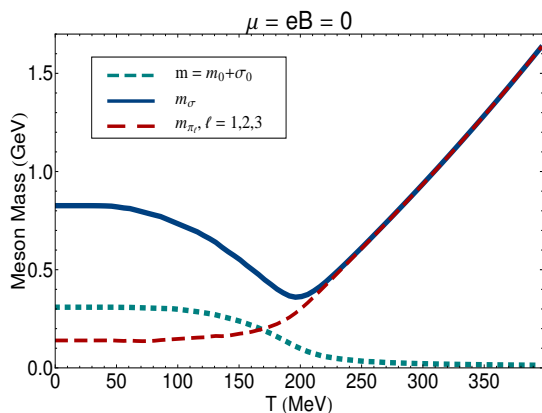


FIG. 2: The T dependence of σ and π meson masses is demonstrated at $\mu = 0$ and for a vanishing magnetic field (solid line for m_σ and dashed line for m_π). Comparing these curves with the T dependence of the constituent quark mass $m = m_0 + \sigma_0$ (dotted line) shows that a mass degeneracy between m_σ and m_π occurs in the chirally restored phase $T > 220 \text{ MeV}$.

Comparing $T_{\text{diss.}}$ and T_{Mott} for different nonvanishing eB in Table I, it seems that the crossover region is shifted to higher temperatures for increasing eB . In the chiral limit, where $T_{\text{diss.}} = T_{\text{Mott}} = T_c$, as mentioned above, this would mean that the critical temperature increases with increasing eB . This phenomenon is related to the magnetic catalysis of dynamical chiral symmetry breaking in the presence of external magnetic fields. Recent lattice results [25] show, however, a certain discrepancy with this conclusion. As it is shown in [25], for certain eB , the critical temperature decreases with increasing eB . This shows that the m dependence of T_c is indeed not trivial. There are a number of attempts in the literature to resolve this disagreement [26, 27], and to explain the so-called inverse magnetic catalysis [28]. Note, that, to the best of our knowledge, inverse magnetic

catalysis was first observed in [29] within a two-flavor NJL model. In one of our previous papers [30], we have also plotted the T - eB phase diagram for different fixed chemical potential μ . As it is shown in Fig. 14(a) and (b) of [30] (see also Fig. 2 in [9]), there are some regions in eB in which T_c decreases with increasing eB and the inverse magnetic catalysis occurs.

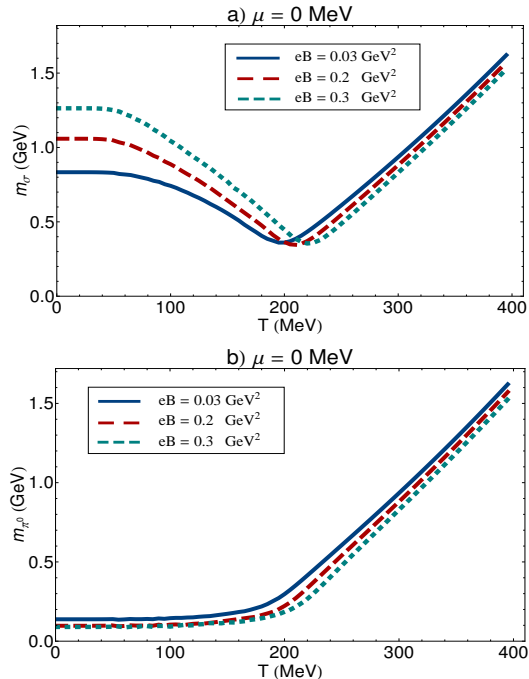


FIG. 3: The T dependence of m_σ [panel (a)] and m_{π^0} [panel (b)] is plotted for $eB = 0.03, 0.2, 0.3 \text{ GeV}^2$ and $\mu = 0 \text{ MeV}$.

In Fig. 3, the T dependence of m_σ [Fig. 3(a)] and m_{π^0} [Fig. 3(b)] are plotted for fixed μ and $eB = 0.03, 0.2, 0.3 \text{ GeV}^2$. At a fixed temperature below (above) the crossover region, the σ -meson mass increases (decreases) with increasing eB . In contrast, m_{π^0} decreases with increasing eB in both symmetry broken and restored phases. The qualitative behavior of the T dependence of m_σ and m_{π^0} for $\mu = 0$ remains unchanged for zero and nonzero eB (see Fig. 9 in [9], where the T dependence of m_σ and m_{π^0} is compared). In particular, m_σ and m_{π^0} are degenerate in the symmetry restored phase $T > 220 \text{ MeV}$.

Let us finally consider the directional refraction indices of neutral mesons, $u_M^{(i)}$, $M \in \{\sigma, \pi^0\}$, that appear in the energy dispersion relation (II.31). They are defined in (II.32). In what follows, we will briefly review the results appearing first in our previous paper [9] for $eB \neq 0$ and $T \neq 0$. In Fig. 4, the T dependence of $u_M^{(i)}$ is plotted for fixed $\mu = 0$ and nonvanishing $eB = 0.03, 0.2, 0.3 \text{ GeV}^2$. For $eB \neq 0$, the refraction indices of σ and π^0 mesons in the longitudinal direction with respect to the direction of the external magnetic field turn out to be equal to unity,

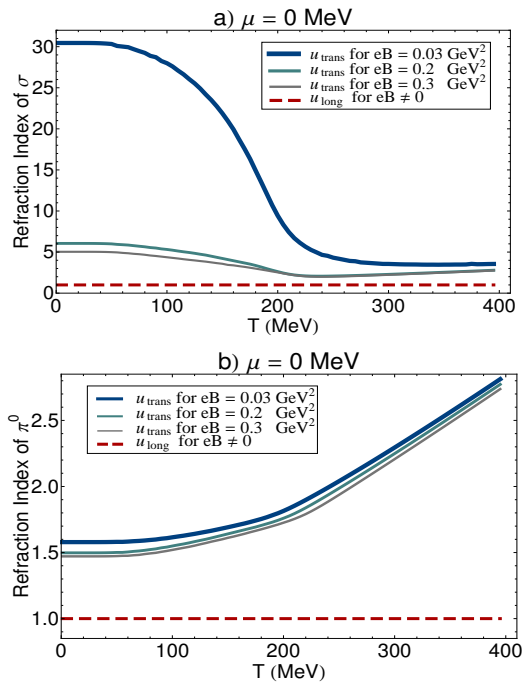


FIG. 4: The T dependence of the transverse and longitudinal refraction indices of σ [panel (a)] and π^0 mesons [panel (b)] is plotted for various eB . The longitudinal refraction index of neutral mesons is equal to unity and independent of T (red dashed lines). In contrast, the transverse refraction index of neutral mesons is larger than unity and decreases with increasing eB . For a B field directed in the third direction, $u_{\text{trans}} \equiv u_M^{(1)} = u_M^{(2)}$ and $u_{\text{long}} \equiv u_M^{(3)}$ for $M \in \{\sigma, \pi^0\}$.

independent of T and μ (see the red dashed lines in Figs. 4(a) and (b)). In the transverse directions, however, the refraction indices of neutral mesons, $u_{\sigma}^{\text{trans}}$ and $u_{\pi^0}^{\text{trans}}$, are T dependent and always larger than unity. It seems that, in the directions perpendicular to the direction of the external magnetic field, the neutral mesons move with a speed larger than the speed of light c . But, this is simply not true. Let us emphasize that, according to the dispersion relation (II.31), this conclusion is only valid for *massless* mesons, where directional group velocities coincide with $u_M^{(i)}$ defined in (II.32). Our mesons are, however, massive,¹⁰ and the fact that the transverse refraction index is larger than unity does not naturally lead to superluminal propagation. Having this in mind, the natural question is what are the consequences of $u_{\sigma}^{\text{trans}} > 1$ and $u_{\pi^0}^{\text{trans}} > 1$? One of our main motivations in this paper, is to answer this interesting question. In the next section, we will show that directional refraction indices play an

important role in the low energy relations of neutral and massive pions, once we have a medium at $T \neq 0$ and/or $eB \neq 0$. But, before coming to this, let us consider again the plots in Fig. 4. As it turns out, for a fixed temperature, u_M^{trans} , $M \in \{\sigma, \pi^0\}$ decrease with increasing eB . This effect is strongly related to the dynamics of fermions in an external magnetic field. As it is stated in [6], for very large magnetic fields, the motion of charged fermions is restricted in directions perpendicular to the magnetic field. A dimensional reduction from $3 + 1$ to $1 + 1$ dimensions occurs in the presence of very strong magnetic fields. Naively, one would expect that the properties of σ and π^0 mesons are not affected by external magnetic fields, simply because they are neutral. But, as is also argued in our previous paper [9], the way we have introduced the background magnetic field in the original Lagrangian (II.1) and the semibosonized Lagrangian (II.3) shows that the effects of the external magnetic field on neutral mesons arise mainly from its interaction with the constituent quarks of these mesonic bound states. According to this argument, the behavior of u_M^{trans} , $M \in \{\sigma, \pi^0\}$ for fixed T and with increasing eB is a realization of the well-established dimensional reduction, appearing mainly in the lowest Landau level (LLL). Note that by increasing the magnetic field strength, the effect of higher Landau levels can be neglected, and the dynamics of fermions is solely determined by LLL, where the above-mentioned dimensional reduction occurs. This is the reason why at a fixed temperature u_M^{trans} , $M \in \{\sigma, \pi^0\}$ decrease with increasing eB . The same property occurs at zero temperature, where the transverse velocity of neutral pions is determined within an effective chiral model in the LLL approximation [27].

Coming back to the plots of Fig. 4, it turns out that for fixed eB , $u_{\sigma}^{\text{trans}}$ decreases with increasing T , while $u_{\pi^0}^{\text{trans}}$ increases with increasing T . The same behavior is also observed for the T dependence of the mass of neutral mesons m_{σ} and m_{π^0} for a fixed eB (see Fig. 2). In this paper, we do not intend to describe the nontrivial relation between u_M^{trans} and m_M , with $M \in \{\sigma, \pi^0\}$. All we want to do is use the neutral pions' directional refraction indices, and study the low energy GT and GOR relations satisfied by these neutral and massive pions. To do this, we will first modify, in the next section, the PCAC relation and prove the GT and GOR relations for $T \neq 0$ and/or $eB \neq 0$ in a model-independent way. In Sec. IV, we will then use the numerical data from the present section to prove the GT and GOR relations in a two-flavor magnetized NJL model at finite T . We will show, in particular, the role played by pions' directional refraction indices in satisfying these relations.

¹⁰ We do not neglect m_0 in our computations. The original theory is therefore nonchiral. Consequently, the neutral pion is not a massless Goldstone mode of the theory, even in the chirally broken phase.

III. DIRECTIONAL WEAK DECAY CONSTANT OF PIONS IN RANDOM PHASE APPROXIMATION

It is known that finite temperature and/or constant magnetic fields explicitly break the relativistic invariance. One of the main consequences of this explicit Lorentz symmetry breaking is that the massive free particles satisfy nontrivial anisotropic energy dispersion relations, including nontrivial directional energy refraction indices. As concerns the massive neutral pions, the anisotropic energy dispersion relation is given by (II.31) with $M = \pi^0$. Whereas at $T = eB = 0$ all refraction indices are equal to unity, at $T \neq 0$ and $eB = 0$, a single refraction index is defined by $u = u_{\pi^0}^{(1)} = u_{\pi^0}^{(2)} = u_{\pi^0}^{(3)}$, and at $T \neq 0$ and $eB \neq 0$, we have $u_{\pi^0}^{(1)} = u_{\pi^0}^{(2)} \neq u_{\pi^0}^{(3)}$.

It is the purpose of this paper to determine the weak decay constant of neutral pions, f_π , at $T \neq 0$ and $eB \neq 0$. To do this, we will generalize in this section the method presented in [3, 31], where f_π is computed at zero T and eB using a multiflavor NJL model. To do this, we will first review in Sec. III A the method presented in [3, 31], by assuming that pions satisfy ordinary isotropic energy dispersion relations $E_\pi^2 = q_i^2 + m_\pi^2$. Combining the usual PCAC relation and the Feynman integral corresponding to a one-pion-to-vacuum matrix element in a random phase approximation (RPA), we arrive at the main relation leading to f_π at zero (T, μ, eB) . As a by-product the quark-pion coupling constant $g_{qq\pi}$ will also be defined in terms of a quark-antiquark polarization loop, in the pion channel. In [3], it is argued that in the chiral limit $m_0 \rightarrow 0$, f_π and $g_{qq\pi}$ satisfy the GT and GOR relations. We will review the method presented in [31], where these relations are proved in the leading and next-to-leading order $1/N_c$ expansion.

In Sec. III B, we will then generalize the arguments in [3, 31] for free pions satisfying the anisotropic energy dispersion relation, $E_{\pi_\ell}^2 = u_{\pi_\ell}^{(i)2} q_i^2 + m_{\pi_\ell}^2$. To do this, we will first define the directional quark-pion coupling constant $g_{qq\pi_\ell}^{(\mu)}$, $\mu = 0, \dots, 3$, in terms of nontrivial form factors $\mathcal{F}_{\ell\ell}^{\mu\nu}$ and refraction indices $u_{\pi_\ell}^{(\mu)} = (1, u_{\pi_\ell}^{(i)})$. We will then introduce a modified PCAC relation including $\mathcal{F}_{\ell\ell}^{\mu\nu}$, the directional refraction indices $u_{\pi_\ell}^{(\mu)}$ and a dimensionful proportionality factor f_b . The directional decay constant of pions, $f_{\pi_\ell}^{(\mu)}$, is then defined by combining $\mathcal{F}_{\ell\ell}^{\mu\nu}$ and f_b . Following the same method as in Sec. III A, we will eventually arrive at the main relation leading to $f_{\pi_\ell}^{(\mu)}$. We will show that $f_{\pi_\ell}^{(\mu)}$ and $g_{qq\pi_\ell}^{(\mu)}$ satisfy modified GT and GOR relations.



FIG. 5: The Schwinger-Dyson gap equation for the quark propagator in the four-fermi NJL model in the Hartree approximation. The bare (dressed) propagator is denoted by thin (thick) lines.

A. Quark-pion coupling constant and pion decay constant from an isotropic energy dispersion relation

Let us start with the Lagrangian density (II.1) of a two-flavor NJL model with $A_\mu^{\text{ext.}} = 0$. As we have mentioned in the previous section, for sufficiently strong G , this model exhibits, in the chiral limit $m_0 \rightarrow 0$, a dynamical mass generation. The resulting mass gap is determined via minimizing the effective (thermodynamic) potential (free energy), in a mean field approximation. Equivalently, it is given by solving the corresponding Schwinger-Dyson (SD) equation for the quark propagator. In the Hartree approximation, the constituent quark mass m is given by

$$m = m_0 + \Sigma_H, \quad (\text{III.1})$$

where m_0 is the bare quark mass and Σ_H is the self-energy of quarks within the four-Fermi NJL model. In the lowest order perturbative expansion, Eq. (III.1) reduces to $m = m_0 + \sigma_0$, where $\sigma_0 = -2G\langle\bar{\psi}\psi\rangle$ is the quark condensate. This is also consistent with the diagrammatic representation of the SD equation, presented in Fig. 5. The SD relation leads to

$$m = m_0 + \sigma_0 \equiv m_0 + 2iG \int \frac{d^4p}{(2\pi)^4} \text{tr}_{sf_c} S(p). \quad (\text{III.2})$$

Here, $S(p) = (\gamma \cdot p - m)^{-1}$ is the dressed quark propagator. The nontrivial solution of the above integral equation leads to a mass gap $\Delta E = 2m$ in the quark spectrum.

Similarly, mesons are described via a Bethe-Salpeter (BS) equation. In Fig. 6, the BS equation for quark-antiquark scattering is demonstrated in RPA. In this approximation, the quark-antiquark scattering matrix

$$T_M(q^2) = \frac{2G}{1 - 2G\Pi_M(q^2)}, \quad (\text{III.3})$$

is given in terms of the quark-antiquark polarization

$\Pi_M(q^2)$ in the $M \in \{\sigma, \pi\}$ channel

$$\Pi_M(q^2) = i \int d^4x \text{tr}_{sf_c} [\Gamma_M S(x) \Gamma_M S(-x)] e^{iq \cdot x}. \quad (\text{III.4})$$

Here, $\Gamma_\sigma = 1$ and $\Gamma_{\pi_a} = i\gamma_5 \tau_a$. The scattering matrix $T_M(q^2)$ can equivalently be written as an effective meson exchange between the external quark-antiquark legs [see the left-hand side (l.h.s.) of the relation appearing in Fig. 6],

$$T_M(q^2) = -\frac{g_{qqM}^2}{q^2 - m_M^2}, \quad (\text{III.5})$$

where g_{qqM} is the quark-meson coupling constant and m_M is the meson pole mass. Note that the denominator in (III.5) reflects the isotropic meson energy dispersion relation

$$E_M^2 = q_i^2 + m_M^2, \quad \text{for } M \in \{\sigma, \vec{\pi}\}. \quad (\text{III.6})$$

Equating $T_M(q^2)$ from (III.3) with (III.5) leads to the definition of the quark-meson coupling constant in terms of $\Pi_M(q^2)$,

$$g_{qqM}^{-2} = \left. \frac{d\Pi_M}{dq^2} \right|_{q^2=m_M^2}, \quad (\text{III.7})$$

as well as

$$1 - 2G\Pi_M(q^2 = m_M^2) = 0, \quad (\text{III.8})$$

which is equivalently given by [31]

$$2G\Pi_M(q^2 = 0) = \frac{\sigma_0}{m} \rightarrow 1, \quad \text{for } m_0 \rightarrow 0. \quad (\text{III.9})$$

As it is argued in [31], relations (III.8) and (III.9) are consistent with Hartree approximation (III.1) as well as the RPA scheme. To determine the pion decay constant f_π , we consider the one-pion-to-vacuum

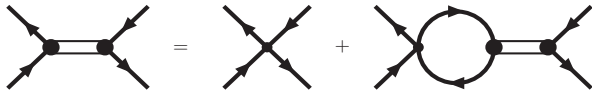


FIG. 6: The Bethe-Salpeter equation for quark-antiquark scattering in RPA [3]. The double lines denote the meson propagator $-(q^2 - m_M^2)^{-1}$ appearing in (III.5), and the solid lines indicate the dressed quark propagators $S(p) = (\gamma \cdot p - m)^{-1}$, including the constituent quark mass m . Fat vertices denote the quark-meson coupling constant defined in (III.7).



FIG. 7: One-pion-to-vacuum matrix element, $\langle 0 | J_{\mu,5}^a(0) | \pi^b(q) \rangle$, in RPA, leading to pion decay constant. Here, $J_{\mu,5}^a \equiv \bar{\psi} \gamma_\mu \gamma_5 \lambda^a \psi$ is the axial vector current, with $\lambda^a \equiv \tau^a/2$. The solid lines are the dressed quark propagator, $S(p) = (\gamma \cdot p - m)^{-1}$, including the constituent quark mass m . The quark-pion coupling $g_{qq\pi_a}$ (fat vertex) is given in (III.7).

matrix element $\langle 0 | J_{\mu,5}^a(0) | \pi^b(q) \rangle$, which satisfies the usual PCAC relation¹¹

$$\langle 0 | J_{\mu,5}^a(0) | \pi^b(q) \rangle = f_\pi q_\mu \delta^{ab}. \quad (\text{III.10})$$

Here, $J_{\mu,5}^a \equiv \bar{\psi} \gamma_\mu \gamma_5 \lambda^a \psi$ with $\lambda^a \equiv \tau^a/2$ is the axial vector current of an axial $SU(2_f)$ global transformation. The matrix element appearing on the r.h.s. of (III.10) is demonstrated diagrammatically in Fig. 7. Note that in RPA, the quark propagator appearing in the quark-antiquark loop in Fig. 7 is the dressed quark propagator $S(p) = (\gamma \cdot p - m)^{-1}$, including the constituent quark mass m . Combining the PCAC relation (III.10) and the Feynman integral corresponding to the one-pion-to-vacuum amplitude demonstrated in Fig. 7, we arrive at

$$f_\pi q_\mu \delta^{ab} = g_{qq\pi} \Upsilon_\mu^{ab}(q), \quad (\text{III.11})$$

with

$$\Upsilon_\mu^{ab}(q) \equiv i \int d^4x \text{tr}_{sf_c} [\gamma_\mu \gamma_5 \lambda^a S(x) \gamma_5 \tau^b S(-x)] e^{iq \cdot x}. \quad (\text{III.12})$$

Contracting (III.11) with q^μ and using the energy dispersion relation (pion on-mass-shell condition) $q^2 = m_\pi^2$, we arrive finally at f_π in terms of $g_{qq\pi}$ and $\Upsilon_\mu^{ab}(q)$. As it is shown in [31], f_π satisfies the GT relation

$$g_{qq\pi} f_\pi = m + \mathcal{O}(m_0^2), \quad (\text{III.13})$$

and the GOR relation

$$m_\pi^2 f_\pi^2 = \frac{m_0 \sigma_0}{2G} + \mathcal{O}(m_0^2), \quad (\text{III.14})$$

¹¹ For $eB = 0$, because of the Lorentz and isospin symmetry of the original Lagrangian, there is no difference between the properties of different species of pions π_ℓ , $\ell = 1, 2, 3$. In so far, we will skip the indices $\ell = 1, 2, 3$ on π_ℓ as long as these symmetries hold.

up to second order in m_0 . Let us emphasize again that the isotropic energy dispersion relation (III.6) plays an important role in proving (III.13) and (III.14) (see [31] for more details). In the next section, we will show how the above relations shall be modified, when we start from a nontrivial anisotropic energy dispersion relation $q_0^2 = u_{\pi_\ell}^{(i)2} q_i^2 + m_{\pi_\ell}^2$ for free $\pi_\ell, \ell = 1, 2, 3$ mesons. In Sec. IV, we will use the results arising from this general consideration to determine the directional quark-pion coupling constant and decay constant for neutral pions in a hot and magnetized medium.

B. Directional quark-pion coupling constant and pion decay constant from an anisotropic energy dispersion relation

Let us consider the Lagrangian density

$$\mathcal{L}_{\pi_\ell} = -\frac{1}{2}\Pi_\ell(x) \left(m_{\pi_\ell}^2 + g^{\mu\mu} u_{\pi_\ell}^{(\mu)2} \partial_\mu^2 \right) \Pi_\ell(x), \quad (\text{III.15})$$

for each pion species $\pi_\ell, \ell = 1, 2, 3$. The above Lagrangian density is comparable to the Lagrangian of pion fields appearing in the effective action (II.15) for free mesons and leads to a nontrivial anisotropic energy dispersion relation

$$E_{\pi_\ell}^2 = u_{\pi_\ell}^{(i)2} q_i^2 + m_{\pi_\ell}^2, \quad \forall \ell = 1, 2, 3, \quad (\text{III.16})$$

similar to (II.31). In (III.15), we have introduced the “normalized” pion field $\Pi_\ell(x) \equiv |\mathcal{F}_{\ell\ell}^{00}|^{1/2} \pi_\ell(x)$, where the form factors $\mathcal{F}_{\ell\ell}^{00}$ appear in the effective action (II.15). Moreover, in analogy to (II.32) and (II.33), the mass m_{π_ℓ} and a four-vector for the refraction index, $u_{\pi_\ell}^{(\mu)}$, for each pion species $\ell = 1, 2, 3$, are defined by the pion mass squared matrix $M_{\pi_\ell}^2$ and form factors $\mathcal{F}_{\ell\ell}^{\mu\nu}$,

$$m_{\pi_\ell} \equiv \left| \frac{M_{\pi_\ell}^2}{\mathcal{F}_{\ell\ell}^{00}} \right|^{1/2}, \quad u_{\pi_\ell}^{(\mu)} \equiv (1, u_{\pi_\ell}^{(i)}) = \left| \frac{\mathcal{F}_{\ell\ell}^{\mu\mu}}{\mathcal{F}_{\ell\ell}^{00}} \right|^{1/2}. \quad (\text{III.17})$$

Using \mathcal{L}_{π_ℓ} from (III.15), the pion propagator $D_{\pi_\ell}(x, y) \equiv \langle 0|T(\pi_\ell(x)\pi_\ell(y))|0\rangle$ in the momentum space reads

$$\tilde{D}_{\pi_\ell}(q) = -\frac{|\mathcal{F}_{\ell\ell}^{00}|^{-1}}{q_0^2 - u_{\pi_\ell}^{(i)2} q_i^2 - m_{\pi_\ell}^2}. \quad (\text{III.18})$$

The metric $g = \text{diag}(1, -1, -1, -1)$. In contrast to (III.5), the denominator reflects the anisotropic pion on-mass-shell condition

$$q_0^2 - u_{\pi_\ell}^{(i)2} q_i^2 = m_{\pi_\ell}^2, \quad \forall \ell = 1, 2, 3, \quad (\text{III.19})$$

including the directional refraction indices $u_{\pi_\ell}^{(i)}$. The factor $|\mathcal{F}_{\ell\ell}^{00}|^{-1}$ in (III.18) arises from the normalization of pion fields, as the pion propagator can equivalently be defined by $D_{\Pi_\ell}(x, y) \equiv \langle 0|T(\Pi_\ell(x)\Pi_\ell(y))|0\rangle$ with

$D_{\Pi_\ell} = |\mathcal{F}_{\ell\ell}^{00}| D_{\pi_\ell}$. Using (III.18), the quark-antiquark scattering amplitude $T_M(q^2)$ from (III.5) with $M = \pi_\ell$ is then modified as

$$T_{\pi_\ell}(q^2) = -\frac{g_{qq\pi_\ell}^2 |\mathcal{F}_{\ell\ell}^{00}|^{-1}}{g^{\mu\mu} u_{\pi_\ell}^{(\mu)2} q_\mu^2 - m_{\pi_\ell}^2}. \quad (\text{III.20})$$

Combining the “bare” quark-pion coupling constant $g_{qq\pi_\ell}$ and the normalization parameter (form factor) $|\mathcal{F}_{\ell\ell}^{00}|$ appearing also in the definition of normalized pion fields, a “normalized” coupling constant $g_{qq\Pi_\ell}$ is defined as

$$g_{qq\Pi_\ell} \equiv g_{qq\pi_\ell} |\mathcal{F}_{\ell\ell}^{00}|^{-1/2}. \quad (\text{III.21})$$

Equating, at this stage, $T_{\pi_\ell}(q^2)$ from (III.20) and the quark-antiquark scattering amplitude from (III.3) with $M = \pi_\ell$, we arrive first at

$$g^{\mu\mu} \frac{d\Pi_{\pi_\ell}(q^2)}{dq_\mu^2} \Big|_{\tilde{q}_{\pi_\ell} = (m_{\pi_\ell}, \mathbf{0})} = u_{\pi_\ell}^{(\mu)2} |\mathcal{F}_{\ell\ell}^{00}| g_{qq\pi_\ell}^{-2}, \quad (\text{III.22})$$

$\forall \mu = 0, \dots, 3$ and $\forall \ell = 1, 2, 3$. Note that in contrast to (III.7), the expression on the l.h.s. of (III.22) is to be evaluated in the rest frame of ℓ th pion species, i.e. in $\tilde{q}_{\pi_\ell} = (m_{\pi_\ell}, \mathbf{0})$. Defining, at this stage, a directional quark-pion coupling constant $g_{qq\pi_\ell}^{(\mu)}$ by

$$(g_{qq\pi_\ell}^{(\mu)}(\tilde{q}_{\pi_\ell}))^{-2} \equiv g^{\mu\mu} \frac{d\Pi_{\pi_\ell}(q^2)}{dq_\mu^2} \Big|_{\tilde{q}_{\pi_\ell} = (m_{\pi_\ell}, \mathbf{0})}, \quad (\text{III.23})$$

plugging this definition into the l.h.s. of (III.22), and using (III.17), we get

$$g_{qq\pi_\ell}^{(\mu)} = g_{qq\pi_\ell} |\mathcal{F}_{\ell\ell}^{\mu\mu}|^{-1/2}. \quad (\text{III.24})$$

Similarly, the directional quark-sigma meson coupling constant is defined by

$$(g_{qq\sigma}^{(\mu)}(\tilde{q}_\sigma))^{-2} \equiv g^{\mu\mu} \frac{d\Pi_\sigma(q^2)}{dq_\mu^2} \Big|_{\tilde{q}_\sigma = (m_\sigma, \mathbf{0})}. \quad (\text{III.25})$$

It satisfies

$$g_{qq\sigma}^{(\mu)} = g_{qq\sigma} |\mathcal{G}^{\mu\mu}|^{-1/2}. \quad (\text{III.26})$$

As it turns out, the directional coupling constant $g_{qq\pi_\ell}^{(\mu)}$ from (III.23) plays a crucial role in the definition of the directional weak decay constant of pions. This is determined by introducing the modified PCAC relation, which shall replace (III.10), whenever pions satisfy the anisotropic energy dispersion relation (III.16),

$$\langle 0|J_{\mu,5}^\ell(0)|\Pi^m(q)\rangle = f_\ell |\mathcal{F}_{\ell\ell}^{00}|^{1/2} u_{\pi_\ell}^{(\mu)2} q_\mu \delta^{\ell m}, \quad (\text{III.27})$$

$\forall \mu = 0, \dots, 3$ and $\forall \ell, m = 1, 2, 3$. Here, f_ℓ is an unknown dimensionful constant, which depends on (T, μ, eB) , whenever they are nonvanishing. Later, we will show that, for neutral pions in the chiral limit

$m_0 \rightarrow 0$, $f_3 = \sigma_0$, where σ_0 is the chiral condensate. For nonvanishing m_0 , we get $f_3 = m$, where $m = m_0 + \sigma_0$. Note that in the chiral limit, where pions are (massless) Goldstone bosons, Eq. (III.27) leads to

$$0 = \langle 0 | \partial^\mu J_{\mu,5}^\ell(0) | \Pi^m(q) \rangle = f_\ell | \mathcal{F}_{\ell\ell}^{00} |^{1/2} m_{\pi_\ell}^2 \delta^{\ell m}, \quad (\text{III.28})$$

in accordance with the Goldstone theorem. Here, the pion on-mass-shell condition (III.19) and the axial $SU(2_f)$ invariance, $\partial^\mu J_{\mu,5}^\ell(x) = 0$, are used. Using the Feynman diagram appearing in Fig. 7 for normalized pion fields, Π_ℓ , the one-pion-to-vacuum matrix element $\langle 0 | J_{\mu,5}^\ell(0) | \Pi^m(q) \rangle$ on the l.h.s. of (III.27) is given by

$$\langle 0 | J_{\mu,5}^\ell(0) | \Pi^m(q) \rangle = g_{qq\Pi_\ell} \Upsilon_\mu^{\ell m}(q), \quad (\text{III.29})$$

where $g_{qq\Pi_\ell}$ and $\Upsilon^{\ell m}(q)$ are given in (III.21) and (III.12), respectively. Relation (III.29) leads, upon using (III.21) and (III.24), as well as the modified PCAC relation (III.27), to

$$f_{\pi_\ell}^{(\mu)} q_\mu \delta^{\ell m} = g_{qq\pi_\ell}^{(\mu)} \Upsilon_\mu^{\ell m}(q), \quad (\text{III.30})$$

$\forall \mu = 0, \dots, 3$ and $\forall \ell, m = 1, 2, 3$. Here, the directional pion decay constant $f_{\pi_\ell}^{(\mu)}$ for the ℓ th pion species is defined by

$$f_{\pi_\ell}^{(\mu)} \equiv f_\ell | \mathcal{F}_{\ell\ell}^{\mu\mu} |^{1/2}. \quad (\text{III.31})$$

In the next section, we will use (III.30) to determine $f_{\pi_0}^{(\mu)}$ for $\mu = 0, \dots, 3$.

Similar to the previous section, the directional quark-pion coupling and decay constants satisfy the modified GT and GOR relations,

$$f_{\pi_\ell}^{(\mu)} g_{qq\pi_\ell}^{(\mu)} = m + \mathcal{O}(m_0^2), \quad (\text{III.32})$$

and

$$m_{\pi_\ell}^2 f_{\pi_\ell}^{(\mu)2} = u_{\pi_\ell}^{(\mu)2} \frac{m_0 \sigma_0}{2G} + \mathcal{O}(m_0^2), \quad (\text{III.33})$$

where $u_{\pi_\ell}^{(\mu)}$ is defined in (III.17). To prove these relations, we generalize the method described in [31] for the case when pions satisfy nontrivial, anisotropic energy dispersion relation (III.16).

As concerns (III.32), let us consider the modified PCAC relation (III.27) and combine it with (III.29). Differentiating the l.h.s. of (III.27) and using [3]

$$\sum_{\mu=0}^3 q^\mu \Upsilon_\mu^{\ell\ell}(q) = m [\Pi_{\pi_\ell}(q^2) - \Pi_{\pi_\ell}(0)], \quad (\text{III.34})$$

with the quark-antiquark polarization, $\Pi_{\pi_\ell}(q^2)$ from (III.4), and $\Upsilon_\mu^{\ell m} = \Upsilon_\mu^{\ell\ell} \delta^{\ell m}$ from (III.12), we first get

$$f_\ell | \mathcal{F}_{\ell\ell}^{00} | m_{\pi_\ell}^2 = m g_{qq\pi_\ell} [\Pi_{\pi_\ell}(q^2) - \Pi_{\pi_\ell}(0)]. \quad (\text{III.35})$$

Expanding $\Pi_{\pi_\ell}(q^2)$ on the r.h.s. of the above relation around $q = 0$, and evaluating the resulting expression at \tilde{q}_{π_ℓ} , we obtain

$$f_\ell | \mathcal{F}_{\ell\ell}^{00} | = m g_{qq\pi_\ell} \frac{d\Pi_{\pi_\ell}}{dq_0^2} \Big|_{\tilde{q}_{\pi_\ell}=(m_{\pi_\ell}, \mathbf{0})} + \mathcal{O}(m_{\pi_\ell}^4), \quad (\text{III.36})$$

which leads, upon using (III.22) for $\mu = 0$, to

$$g_{qq\pi_\ell} f_\ell = m + \mathcal{O}(m_0^2). \quad (\text{III.37})$$

Plugging (III.24) as well as (III.31) into (III.37), we arrive finally at the GT relation (III.32), including directional quark-pion coupling and pion decay constants. To show the GOR relation (III.33), we use (III.8) in a slightly modified form,

$$1 - 2G\Pi_{\pi_\ell}(\tilde{q}_{\pi_\ell} = (m_{\pi_\ell}, \mathbf{0})) = 0. \quad (\text{III.38})$$

This relation arises, similarly to (III.8), by equating (III.20) and (III.3) with $M = \pi_\ell$. Expanding the l.h.s. of (III.38) around $q^2 = 0$ and evaluating the resulting expression at $\tilde{q}_{\pi_\ell} = (m_{\pi_\ell}, \mathbf{0})$, we get first

$$0 = 1 - 2G\Pi_{\pi_\ell}(0) - 2Gm_{\pi_\ell}^2 \frac{d\Pi_{\pi_\ell}(q^2)}{dq_0^2} \Big|_{\tilde{q}_{\pi_\ell}=(m_{\pi_\ell}, \mathbf{0})} + \mathcal{O}(m_{\pi_\ell}^4), \quad (\text{III.39})$$

which yields

$$m_{\pi_\ell}^2 = \frac{g_{qq\pi_\ell}^2 m_0}{2Gm | \mathcal{F}_{\ell\ell}^{00} |} + \mathcal{O}(m_{\pi_\ell}^4). \quad (\text{III.40})$$

Here, Eq. (III.9) and the definition of $g_{qq\pi_\ell}^{(\mu)}$ from (III.23) are used. Plugging further the GT relation (III.37) and (III.31), as well as the definition of $u_{\pi_\ell}^{(\mu)2}$ from (III.17) into the r.h.s. of (III.40), we arrive finally at the modified GOR relation (III.33), including $f_{\pi_\ell}^{(\mu)}$.

As it turns out, whereas (III.34) plays an important role in proving (III.13) and (III.14), it is not so crucial to derive (III.32) and (III.33). In the next section, we will first use the above results to derive a number of analytical expressions for the directional quark-pion coupling and decay constants for neutral pions. Using these expressions, together with the modified PCAC relation (III.27), we will then analytically prove the GT and GOR relations (III.32) and (III.33), without using (III.34). We will then verify these low energy relations for neutral pions numerically and eventually present numerical results for $g_{qq\pi_0}^{(\mu)}$ and $f_{\pi_0}^{(\mu)}$.

**IV. DIRECTIONAL QUARK-PION
COUPLING AND PION DECAY CONSTANTS
AT FINITE (T, μ, eB)**

A. Analytical results

1. *Directional quark-meson couplings for neutral mesons*

Let us consider the quark-antiquark polarization $\Pi_M(q^2)$ from (III.4) in the $M \in \{\sigma, \pi^0\}$ channel. In the presence of an external magnetic field the fermion propagators $S(x)$ appearing in (III.4) are to be replaced by Ritus propagators, $S_Q(x)$ from (II.24)-(II.27). Plugging (II.24) into (III.4), we arrive first at

$$\begin{aligned} & \Pi_M(q) \\ &= i \sum_{p,k=0}^{\infty} \int \mathcal{D}\tilde{p} \mathcal{D}\tilde{k} \int d^4x e^{-i(\tilde{p}-\tilde{k}-q)\cdot x} \Lambda_{pk}^M(\tilde{p}, \tilde{k}, x_1), \end{aligned} \quad (\text{IV.1})$$

where

$$\begin{aligned} \Lambda_{pk}^M(\tilde{p}, \tilde{k}, x_1) &= \text{tr}_{sfc} [\Gamma_M P_p(x_1) S_Q(\tilde{p}) P_p(0) \Gamma_M \\ &\quad \times K_k(0) S_Q(\tilde{k}) K_k(x_1)]. \end{aligned} \quad (\text{IV.2})$$

Here, $\Gamma_\sigma = 1$ and $\Gamma_{\pi^0} = i\gamma_5\tau^3$, and $\tau^3 = \text{diag}(1, -1)$ is the third Pauli matrix. The momenta \tilde{p} and \tilde{k} are defined below (II.24). In (IV.1), integrating first over x_0, x_2, x_3 and then over p_0, p_2, p_3 components, we arrive at the boundary conditions $p_i = k_i + q_i$ for $i = 0, 2, 3$. In what follows, we will abbreviate these boundary conditions by a subscript ‘‘b.c.’’ Plugging $P_p(x_1)$ from (II.25) into (IV.2), we arrive first at

$$\begin{aligned} \Pi_M(q) &= i \sum_{p,k=0}^{\infty} \int \frac{dk_0 dk_3}{(2\pi)^3} \\ &\quad \times \int dk_2 dx_1 e^{-iq_1 x_1} \Lambda_{pk}^M(\tilde{p}, \tilde{k}, x_1) \Big|_{\text{b.c.}}, \end{aligned} \quad (\text{IV.3})$$

with

$$\Lambda_{pk}^M(\tilde{p}, \tilde{k}, x_1) = -12 \sum_{q_f} \left\{ \frac{\tilde{k}\cdot\tilde{p} + \kappa_M m^2}{(\tilde{p}^2 - m^2)(\tilde{k}^2 - m^2)} [A_{pk}^{+(0)} \alpha_{pk}^+ + A_{pk}^{-(0)} \alpha_{pk}^-] + \frac{2\tilde{p}_2 \tilde{k}_2}{(\tilde{p}^2 - m^2)(\tilde{k}^2 - m^2)} A_{pk}^{-(0)} \alpha_{pk}^- \right\}, \quad (\text{IV.4})$$

where $\kappa_{\pi^0} = -1$ and $\kappa_\sigma = 1$. From the decomposition

$$\begin{aligned} P_p(0) K_k(0) &\equiv \alpha_{pk}^+(p_2, k_2) + is\gamma_1 \gamma_2 \alpha^-(p_2, k_2), \\ K_k(x_1) P_p(x_1) &\equiv A_{pk}^{+(0)}(x_1) + is\gamma_1 \gamma_2 A_{pk}^{-(0)}(x_1), \end{aligned} \quad (\text{IV.5})$$

we have

$$\begin{aligned} \alpha_{pk}^{\pm(0)}(p_2, k_2) &\equiv \frac{1}{2} [f_p^{+s}(0) f_k^{+s}(0) \\ &\quad \pm \Pi_p \Pi_k f_p^{-s}(0) f_k^{-s}(0)], \end{aligned} \quad (\text{IV.6})$$

and

$$\begin{aligned} A_{pk}^{\pm(0)}(x_1) &\equiv \frac{1}{2} [f_p^{+s}(x_1) f_k^{+s}(x_1) \\ &\quad \pm \Pi_p \Pi_k f_p^{-s}(x_1) f_k^{-s}(x_1)]. \end{aligned} \quad (\text{IV.7})$$

In (IV.4), the summation over $q_f \in \{2/3, -1/3\}$ replaces the trace in the flavor space. Moreover, we set $N_c = 3$. In what follows, we will use $\Pi_M(q^2)$ from (IV.3) to derive the directional quark-meson coupling $g_{qqM}^{(\mu)}$, $M \in \{\sigma, \pi^0\}$ in the direction longitudinal, $\mu = (0, 3)$, and transverse, $\mu = (1, 2)$, with respect to the direction of the external magnetic field. Here, the definitions (III.23) with $\ell = 3$ and (III.25), for $(g_{qqM}^{(\mu)}(\tilde{q}_M))^{-2}$, $M \in \{\pi^0, \sigma\}$ in the rest frame of mesons $\tilde{q}_M \equiv (m_M, \mathbf{0})$, will be used.

Using $\Pi_M(q)$ from (IV.3) and plugging $\Lambda_{pk}^M(\tilde{p}, \tilde{k}, x_1)$ from (IV.4) in

$$\begin{aligned} (g_{qqM}^{(\mu)}(\tilde{q}_M))^{-2} &= i \sum_{p,k=0}^{\infty} \int \frac{dk_0 dk_3}{(2\pi)^3} \int dk_2 dx_1 \\ &\quad \times g^{\mu\mu} \frac{d}{dq_\mu^2} \left[e^{-iq_1 x_1} \Lambda_{pk}^M(\tilde{p}, \tilde{k}, x_1) \right] \Big|_{\tilde{q}_M, \text{b.c.}}, \end{aligned} \quad (\text{IV.8})$$

which arises from (III.23) and (III.25), choosing $\mu = 0$, and eventually using

$$\int dk_2 dx_1 A_{pk}^{-(0)} \alpha_{pk}^- \Big|_{p_2=k_2} = \frac{1}{4} |q_f eB| \delta_{p,k} \delta_{k,0}, \quad (\text{IV.9})$$

as well as

$$\begin{aligned} \int dk_2 dx_1 [A_{pk}^{+(0)} \alpha_{pk}^+ + A_{pk}^{-(0)} \alpha_{pk}^-] \Big|_{p_2=k_2} \\ = \frac{1}{2} |q_f eB| \alpha_k \delta_{p,k}, \end{aligned} \quad (\text{IV.10})$$

we arrive first at

$$(g_{qqM}^{(0)}(\tilde{q}_M))^{-2} = 6i \sum_{q_f} |q_f eB| \sum_{k=0}^{\infty} \alpha_k \int_0^1 dx x(1-x) \times \int \frac{dk_0 dk_3}{(2\pi)^3} \left\{ \frac{3}{(\bar{k}^2 + x(1-x)m_M^2 - m^2)^2} - \frac{4\Xi_M(x)}{(\bar{k}^2 + x(1-x)m_M^2 - m^2)^3} \right\}, \quad (\text{IV.11})$$

with

$$\begin{aligned} \Xi_{\pi^0}(x) &\equiv x(1-x)m_{\pi^0}^2, \\ \Xi_{\sigma}(x) &\equiv x(1-x)m_{\sigma}^2 - m^2, \end{aligned} \quad (\text{IV.12})$$

for a nonzero magnetic field and at $T = \mu = 0$. In the above relations $\bar{k}^2 = \mathbf{k}_{\parallel}^2 - 2|q_f eB|k$ with $\mathbf{k}_{\parallel}^2 = k_0^2 - k_3^2$. To derive (IV.9) and (IV.10), we use the same technique, developed in [9] (A number of useful relations, that can be used to derive (IV.9) and (IV.10) are presented in the Appendix). At finite (T, μ, eB) , we obtain

$$(g_{qqM}^{(0)}(\tilde{q}_M))^{-2} = -6 \sum_{q_f} |q_f eB| \sum_{k=0}^{\infty} \alpha_k \int_0^1 dx x(1-x) \times \int \frac{dk_3}{(2\pi)^2} \left\{ 3\mathcal{S}_2^{(0)}(\omega_k^M(x)) - 4\Xi_M(x)\mathcal{S}_3^{(0)}(\omega_k^M(x)) \right\}, \quad (\text{IV.13})$$

where $\Xi_M(x)$ is given in (IV.12). To introduce (T, μ) , Eq. (II.28) is used. In the above relations $\omega_k^M(x)$, $M \in \{\sigma, \pi^0\}$ is defined by

$$\omega_k^M(x) \equiv [k_3^2 + 2|q_f eB|k - x(1-x)m_M^2 + m^2]^{1/2}. \quad (\text{IV.14})$$

Moreover, similar to the computation presented in [9], we have used the functions

$$\mathcal{S}_{\ell}^{(m)}(\omega) \equiv T \sum_{n=-\infty}^{+\infty} \frac{(k_0^2)^m}{(k_0^2 - \omega^2)^{\ell}}, \quad (\text{IV.15})$$

with $\ell \geq 1, m \geq 0$. Using

$$\mathcal{S}_1^{(0)}(\omega) = \frac{1}{2\omega} [1 - N_f(\omega)], \quad (\text{IV.16})$$

with $N_f(\omega) \equiv n_f^+(\omega) + n_f^-(\omega)$ and the fermion distribution functions

$$n_f^{\pm}(\omega) \equiv \frac{1}{e^{\beta(\omega \mp \mu)} + 1}, \quad (\text{IV.17})$$

the following recursion relations can be used to evaluate $\mathcal{S}_{\ell}^{(m)}(\omega)$, $\forall \ell \geq 1, m \geq 0$,

$$\mathcal{S}_{\ell}^{(0)}(\omega) = \frac{1}{2(\ell-1)\omega} \frac{d\mathcal{S}_{\ell-1}^{(0)}(\omega)}{d\omega}, \quad \ell \geq 2,$$

$$\mathcal{S}_{\ell}^{(m)}(\omega) = \mathcal{S}_{\ell-1}^{(m-1)}(\omega) + \omega^2 \mathcal{S}_{\ell}^{(m-1)}(\omega). \quad (\text{IV.18})$$

In Sec. IV B, we will numerically evaluate the sum over Landau levels k and the integration over k_3 momentum, appearing in (IV.13).

To determine $(g_{qqM}^{(1)}(\tilde{q}_M))^{-2}$, we use (IV.8) with $\mu = 1$. To compute the differentiation with respect to q_1^2 , we use the identity $\frac{df(q_1)}{dq_1^2}|_{\tilde{q}_M, \text{b.c.}} = \frac{1}{2} \frac{d^2 f(q_1)}{dq_1^2}|_{\tilde{q}_M, \text{b.c.}}$, which is correct for $\tilde{q}_M = (m_M, \mathbf{0})$. The integration over k_2 and x_1 can be carried out using

$$\int dk_2 dx_1 x_1 A_{pk}^{\pm(0)} \alpha_{pk}^{\pm} \Big|_{p_2=k_2} = 0. \quad (\text{IV.19})$$

We arrive first at

$$(g_{qqM}^{(1)}(\tilde{q}_M))^{-2} = \frac{i}{2} \sum_{p,k=0}^{\infty} \int \frac{dk_0 dk_3}{(2\pi)^3} \times \int dk_2 dx_1 e^{-iq_1 x_1} x_1^2 \Lambda_{pk}^M(\bar{p}, \bar{k}, x_1) \Big|_{\tilde{q}_M, \text{b.c.}}, \quad (\text{IV.20})$$

for $M \in \{\sigma, \pi^0\}$. Plugging (IV.4) into (IV.20), and using

$$\begin{aligned} \int dk_2 dx_1 x_1^2 [A_{pk}^{+(0)} \alpha_{pk}^+ + A_{pk}^{-(0)} \alpha_{pk}^-] \Big|_{p_2=k_2} &= \frac{1}{2} C_{pk}^{(1)}, \\ \int dk_2 dx_1 x_1^2 A_{pk}^{-(0)} \alpha_{pk}^- \Big|_{p_2=k_2} &= -\frac{1}{4} C_{pk}^{(2)}, \end{aligned} \quad (\text{IV.21})$$

with $C_{pk}^{(i)}$, $i = 1, 2$, defined by

$$\begin{aligned} C_{pk}^{(1)} &= \delta_{p,k} (4k + \delta_{k,0}) - \Pi_k (2k-1) \delta_{p,k-1} \\ &\quad - (2k+1) \delta_{p,k+1}, \\ C_{pk}^{(2)} &= -\delta_{p,k} \delta_{k,0} + \Pi_k \left(2k-1 - 2\sqrt{k(k-1)} \right) \delta_{p,k-1} \\ &\quad + \left(2k+1 - 2\sqrt{k(k+1)} \right) \delta_{p,k+1}, \end{aligned} \quad (\text{IV.22})$$

we first arrive for $B \neq 0$ and at $T = \mu = 0$, at

$$(g_{qqM}^{(1)}(\tilde{q}_M))^{-2} = -3i \sum_{q_f} \sum_{p,k=0}^{\infty} \int_0^1 dx \int \frac{dk_0 dk_3}{(2\pi)^3} \left\{ \frac{[\mathbf{k}_{\parallel}^2 - x(1-x)m_M^2 - \Delta_{pk}^{(M)}]}{[\mathbf{k}_{\parallel}^2 + x(1-x)m_M^2 - \Delta_{pk}]^2} C_{pk}^{(1)} - \frac{\bar{p}_2 \bar{k}_2}{[\mathbf{k}_{\parallel}^2 + x(1-x)m_M^2 - \Delta_{pk}]^2} C_{pk}^{(2)} \right\}, \quad (\text{IV.23})$$

with

$$\begin{aligned} \Delta_{pk}^{\pi^0} &\equiv 2|q_f eB| \sqrt{pk} + m^2, \\ \Delta_{pk}^{\sigma} &\equiv 2|q_f eB| \sqrt{pk} - m^2, \\ \Delta_{pk} &\equiv 2|q_f eB| [(1-x)k + xp] + m^2. \end{aligned} \quad (\text{IV.24})$$

At finite (T, μ, eB) , we therefore have

$$(g_{qqM}^{(1)}(\tilde{q}_M))^{-2} = 3 \sum_{q_f} \sum_{k=0}^{\infty} \int_0^1 dx \int \frac{dk_3}{(2\pi)^2} \left\{ (4k + \delta_{k0}) [\mathcal{S}_1^{(0)}(\omega_k^M(x)) - 2\Xi_M(x) \mathcal{S}_2^{(0)}(\omega_k^M(x))] - 2(2k+1) [\mathcal{S}_1^{(0)}(\omega_{k+x}^M(x)) - 2\Xi_M(x) \mathcal{S}_2^{(0)}(\omega_{k+x}^M(x))] + 4|qeB| (k-x-2kx) \mathcal{S}_2^{(0)}(\omega_{k+x}^M(x)) \right\}, \quad (\text{IV.25})$$

where $\Xi_M(x)$ and $\omega_k^M(x)$ are defined in (IV.12) and (IV.14), respectively. In the Appendix, we will present the method we have used to sum over p in (IV.23) and to arrive at (IV.25).

As concerns $(g_{qqM}^{(2)}(\tilde{q}_M))^{-2}$, we set $\mu = 2$ in (IV.8). Using $\frac{df(q_2)}{dq_2^2}|_{\tilde{q}_M, \text{b.c.}} = \frac{1}{2} \frac{d^2 f(q_2)}{dq_2^2}|_{\tilde{q}_M, \text{b.c.}}$ and

$$\int dx_1 dk_2 \frac{d^2}{dq_2^2} \left(A_{pk}^{+(0)} \alpha_{pk}^+ + A_{pk}^{-(0)} \alpha_{pk}^- \right) \Big|_{p_2=k_2} = -\frac{1}{2} C_{pk}^{(1)}, \quad \int dx_1 dk_2 \frac{d^2}{dq_2^2} A_{pk}^{-(0)} \alpha_{pk}^- \Big|_{p_2=k_2} = \frac{1}{4} C_{pk}^{(2)}, \quad (\text{IV.26})$$

with $C_{pk}^{(i)}$, $i = 1, 2$ given in (IV.22), and eventually plugging these relations into the resulting expression, it turns out that

$$g_{qqM}^{(1)}(\tilde{q}_M) = g_{qqM}^{(2)}(\tilde{q}_M), \quad \text{for } M \in \{\sigma, \pi^0\}. \quad (\text{IV.27})$$

At finite (T, μ, eB) , the inverse squared value of $g_{qqM}^{(1)}(\tilde{q}_M)$ is given in (IV.25). In the Appendix, we will present the necessary relations that can be used to derive (IV.26). To derive $g_{qqM}^{(3)}(\tilde{q}_M)$, we set $\mu = 3$ in (IV.8). Using (IV.9) and (IV.10), we arrive at

$$g_{qqM}^{(0)}(\tilde{q}_M) = g_{qqM}^{(3)}(\tilde{q}_M), \quad \text{for } M \in \{\sigma, \pi^0\}, \quad (\text{IV.28})$$

where, at finite (T, μ, eB) , the inverse squared value of $g_{qqM}^{(0)}(\tilde{q}_M)$ is given in (IV.13). Note that, at this stage, in the limit of $m_{\pi} \rightarrow 0$, $g_{qq\sigma}^{(\mu)}(\tilde{q}_{\sigma})$ and $g_{qq\pi^0}^{(\mu)}(\tilde{q}_{\pi^0})$, arising in (IV.13) and (IV.25), as well as (IV.27) and (IV.28), satisfy $g_{qq\sigma}^{(\mu)} = |\mathcal{G}^{\mu\mu}|^{-1/2}$ as well as $g_{qq\pi^0}^{(\mu)} = |\mathcal{F}_{33}^{\mu\mu}|^{-1/2}$. Here, the analytical expressions of $\mathcal{G}^{\mu\mu}$ and $\mathcal{F}_{33}^{\mu\mu}$ are explicitly presented in [9]. This is indeed expected from (III.24) and (III.26), which are valid for arbitrary meson masses m_{σ} and m_{π^0} . This shows that g_{qqM} , $M \in \{\sigma, \pi^0\}$ arising in (III.24) and (III.26) are, in the limit $m_M \rightarrow 0$, equal to unity. In Sec.

IV B, we will evaluate numerically the k_3 integration and the summation over Landau levels k , which appear in (IV.13) as well as (IV.25). We will present the T dependence of directional quark-meson couplings $g_{qqM}^{(\mu)}$, $\mu = 0, \dots, 3$, and $M \in \{\sigma, \pi^0\}$ at zero chemical potential and for $eB = 0.03, 0.2, 0.3 \text{ GeV}^2$. We will, in particular, verify (III.24) for all T -dependent pion masses. Moreover, we will use the data arising from these results for $g_{qqM}^{(\mu)}$, $\mu = 0, \dots, 3$, to determine the T dependence of directional decay constants of neutral pions, $f_{\pi^0}^{(\mu)}$, $\mu = 0, \dots, 3$, at zero chemical potential and for finite and fixed magnetic fields. In what follows, we will present the analytical results for $f_{\pi^0}^{(\mu)}$, $\mu = 0, \dots, 3$, using (III.30) with $\ell = m = 3$.

2. Directional pion decay constant for neutral pions

Let us consider (III.30) with $\ell = 3$ for neutral pions. Using the fact that $\Upsilon_{\mu}^{\ell m}(q) = \delta_{\ell m} \Upsilon_{\mu}^{\ell\ell}$, $\forall \ell, m = 1, 2, 3$, with $\Upsilon_{\mu}^{\ell m}$ given in (III.12), and setting $\ell = 3$, we get

$$f_{\pi^0}^{(\mu)} q_{\mu} = g_{qq\pi^0}^{(\mu)} \Upsilon_{\mu}^{33}(q). \quad (\text{IV.29})$$

As it turns out, Eq. (IV.29) is not appropriate to determine $f_{\pi^0}^{(\mu)}$ in the rest frame of neutral mesons,

especially in the spatial directions. Later we will show that this is mainly because the spatial components of $\Upsilon_\mu^{33}(q)$ vanish in the rest frame of neutral mesons, i.e. $\Upsilon_i^{33}(\tilde{q}_{\pi^0}) = 0$ for $\tilde{q}_{\pi^0} = (m_{\pi^0}, \mathbf{0})$. In what follows, after determining $\Upsilon_\mu^{33}(q)$ in the presence of external magnetic fields, we will present a method from which $f_{\pi^0}^{(\mu)}$ can be determined for all $\mu = 0, \dots, 3$.

We start by plugging the Ritus propagators (II.24)-(II.27) into (III.12), to arrive at

$$\begin{aligned} \Upsilon_\mu^{33}(q) &= \frac{i}{2} \sum_{p,k=0}^{\infty} \int \mathcal{D}\tilde{p} \mathcal{D}\tilde{k} \\ &\times \int d^4x e^{-i(\tilde{p}-\tilde{k}-q)\cdot x} \Lambda_{pk}^{(\mu,3)}(\tilde{p}, \tilde{k}, x_1), \end{aligned} \quad (\text{IV.30})$$

with

$$\begin{aligned} \Lambda_{pk}^{(\mu,3)}(\tilde{p}, \tilde{k}, x_1) &= \text{tr}_{sf} [\gamma^\mu P_p(x_1) S_Q(\tilde{p}) P_p(0) \\ &\times i\gamma_5 \tau^3 K_k(0) S_Q(\tilde{k}) K_k(x) i\gamma_5 \tau^3]. \end{aligned} \quad (\text{IV.31})$$

Integrating over x_0, x_2, x_3 , and eventually over p_0, p_2, p_3 components, we arrive at the same boundary conditions $p_i = k_i + q_i, i = 0, 2, 3$, as described in the paragraph following (IV.2). Plugging $P_p(x_1)$ from (II.25) into (IV.31), and using the decomposi-

tion $P_p(0)K_k(0)$, as given in (IV.5), and

$$\begin{aligned} K_k(x_1)\gamma^\mu P_p(x_1) \\ = \gamma^\mu [(A_{pk}^{+(\mu)}(x_1) + is\gamma_1\gamma_2 A_{pk}^{-(\mu)}(x_1)], \end{aligned} \quad (\text{IV.32})$$

with

$$\begin{aligned} A_{pk}^{\pm(0)} &= A_{pk}^{\pm(3)} \\ &= \frac{1}{2} [f_p^{+s}(x_1) f_k^{+s}(x_1) \pm \Pi_p \Pi_k f_p^{-s}(x_1) f_k^{-s}(x_1)], \\ A_{pk}^{\pm(1)} &= A_{pk}^{\pm(2)} \\ &= \frac{1}{2} [\Pi_k f_p^{+s}(x_1) f_k^{-s}(x_1) \pm \Pi_p f_p^{-s}(x_1) f_k^{+s}(x_1)], \end{aligned} \quad (\text{IV.33})$$

we arrive at

$$\begin{aligned} \Upsilon_\mu^{33}(q) &= \frac{i}{2} \sum_{p,k=0}^{\infty} \int \frac{dk_0 dk_3}{(2\pi)^3} \\ &\times \int dk_2 dx_1 e^{-iq_1 \cdot x_1} \Lambda_{pk}^{(\mu,3)}(\tilde{p}, \tilde{k}, x_1) \Big|_{\text{b.c.}}, \end{aligned} \quad (\text{IV.34})$$

with

$$\Lambda_{pk}^{(\mu,3)}(\tilde{p}, \tilde{k}, x_1) = 12m \sum_{q_f} \left\{ \frac{(\tilde{p} - \tilde{k})_\mu \mathcal{N}_{pk}^{(\mu)} - isg\mu^1 [\tilde{k}_2 \mathcal{M}_{pk}^{+(\mu)} + \tilde{p}_2 \mathcal{M}_{pk}^{-(\mu)}] + 2g\mu^2 \tilde{p}_2 \mathcal{P}_{pk}^{(\mu)}}{(\tilde{p}^2 - m^2)(\tilde{k}^2 - m^2)} \right\}, \quad (\text{IV.35})$$

and

$$\mathcal{N}_{pk}^{(\mu)} \equiv A_{pk}^{+(\mu)} \alpha_{pk}^+ + A_{pk}^{-(\mu)} \alpha_{pk}^-, \quad \mathcal{M}_{pk}^{\pm(\mu)} \equiv A_{pk}^{+(\mu)} \alpha_{pk}^- \pm A_{pk}^{-(\mu)} \alpha_{pk}^+, \quad \mathcal{P}_{pk}^{(\mu)} = \alpha_{pk}^- A_{pk}^{-(\mu)}. \quad (\text{IV.36})$$

Using (IV.10) as well as

$$\int dk_2 dx_1 A_{pk}^{\pm(1)} \alpha_{pk}^\pm \Big|_{p_2=k_2} = 0, \quad \int dk_2 dx_1 A_{pk}^{\pm(1)} \alpha_{pk}^\mp \Big|_{p_2=k_2} = 0, \quad (\text{IV.37})$$

and performing the integration over k_2 and x_1 in (IV.34) for $q = \tilde{q}_{\pi^0}$, we get

$$\Upsilon_i^{33}(\tilde{q}_{\pi^0}) = 0, \quad \text{for } i = 1, 2, 3. \quad (\text{IV.38})$$

Thus, in order to determine $f_{\pi^0}^{(\mu)}$ from (IV.29), especially in the spatial directions, we have to expand the r.h.s. of (IV.29) around \tilde{q}_{π^0} , and then evaluate both sides at \tilde{q}_{π^0} . Keeping in mind that $g_{qq\pi^0}^{(\mu)}$, appearing on the r.h.s. of (IV.29) and defined in (III.23), depends, in general, on q , we obtain

$$f_{\pi^0}^{(0)} = m_{\pi^0}^{-1} g_{qq\pi^0}^{(0)}(\tilde{q}_{\pi^0}) \Upsilon_0^{33}(\tilde{q}_{\pi^0}), \quad (\text{IV.39})$$

$$f_{\pi^0}^{(i)} = g_{qq\pi^0}(\tilde{q}_{\pi^0}) \frac{d}{dq_i} \Upsilon_i^{33}(\tilde{q}_{\pi^0}), \quad (\text{IV.40})$$

for $i = 1, 2, 3$. In what follows, Eqs. (IV.39) and (IV.40) will be used to determine the analytical expressions for $f_{\pi^0}^{(\mu)}, \mu = 0, \dots, 3$.

Setting $\mu = 0$ in (IV.34) with $\Lambda_{pk}^{(\mu,3)}$ given in (IV.35), and using (IV.10) to evaluate the integration over k_2 and x_1 , $f_{\pi^0}^{(0)}$ from (IV.39) reads

$$\begin{aligned} f_{\pi^0}^{(0)} &= 3im g_{qq\pi^0}^{(0)}(\tilde{q}_{\pi^0}) \sum_{k=0}^{\infty} \alpha_k \sum_{q_f} |q_f eB| \\ &\times \int_0^1 dx \int \frac{dk_0 dk_3}{(2\pi)^3} \frac{1}{[\tilde{k}^2 + x(1-x)m_{\pi^0}^2 - m^2]^2}, \end{aligned} \quad (\text{IV.41})$$

for nonzero eB and vanishing T and μ , as well as

$$f_{\pi^0}^{(0)} = -3m g_{qq\pi^0}^{(0)} \sum_{q_f} |q_f eB| \sum_{k=0}^{\infty} \alpha_k \times \int_0^1 dx \int \frac{dk_3}{(2\pi)^2} \mathcal{S}_2^{(0)}(\omega_k^{\pi^0}(x)), \quad (\text{IV.42})$$

at finite (T, μ, eB) . Here, $\mathcal{S}_2^{(0)}(\omega_k^{\pi^0}(x))$ with $\omega_k^{\pi^0}(x)$ from (IV.14) is defined in (IV.15) and can be evaluated using the recursion relations in (IV.18).

Plugging $i = 1$ into (IV.40), we arrive first at

$$f_{\pi^0}^{(1)} = 6im g_{qq\pi^0}^{(1)}(\tilde{q}_{\pi^0}) \sum_{p,k=0}^{\infty} \sum_{q_f} s \int \frac{dk_0 dk_3}{(2\pi)^3} \times \int dk_2 dx_1 \frac{[\bar{k}_2 x_1 \mathcal{M}_{pk}^{+(1)} + \bar{p}_2 x_1 \mathcal{M}_{pk}^{-(1)}]}{(\bar{p}^2 - m^2)(k^2 - m^2)} \Big|_{\tilde{q}_{\pi^0, \text{b.c.}}}, \quad (\text{IV.43})$$

where $\mathcal{M}_{pk}^{\pm(1)}$ are defined in (IV.36) with $\mu = 1$. The integrations over k_2 and x_1 can be performed using

$$\int dk_2 dx_1 x_1 A_{pk}^{\pm(1)} \alpha_{pk}^{\mp} = -\frac{\sqrt{|q_f eB|}}{4\sqrt{2}} \times [\Pi_k \delta_{p,k-1}(\sqrt{k} \mp \sqrt{k-1}) \pm \Pi_{k+1} \delta_{p,k+1}(\sqrt{k+1} \mp \sqrt{k})]. \quad (\text{IV.44})$$

After plugging (IV.44) into (IV.43) and summing over p , by making use of the method described in the Appendix, we arrive, after some work, at

$$f_{\pi^0}^{(1)} = 6im g_{qq\pi^0}^{(1)}(\tilde{q}_{\pi^0}) \sum_{k=0}^{\infty} \sum_{q_f} |q_f eB| \int \frac{dk_0 dk_3}{(2\pi)^3} \times \frac{1}{[\mathbf{k}_{\parallel}^2 + x(1-x)m_{\pi^0}^2 - m^2 - 2|q_f eB|(k+x)]^2}, \quad (\text{IV.45})$$

for nonvanishing eB and at zero (T, μ) . At finite (T, μ, eB) , we therefore get

$$f_{\pi^0}^{(1)} = -6m g_{qq\pi^0}^{(1)}(\tilde{q}_{\pi^0}) \sum_{k=0}^{\infty} \sum_{q_f} |q_f eB| \times \int_0^1 dx \int \frac{dk_3}{(2\pi)^2} \mathcal{S}_2^{(0)}(\omega_{k+x}^{\pi^0}(x)). \quad (\text{IV.46})$$

To determine $f_{\pi^0}^{(2)}$, we use (IV.40) with $i = 2$. Plugging (IV.34)-(IV.35) into the resulting expression, using

$$\int dk_2 dx_1 \alpha_{pk}^{\pm} \frac{d}{dk_2} A_{pk}^{\pm(1)} \Big|_{p_2=k_2} = 0, \quad (\text{IV.47})$$

as well as

$$\int dk_2 dx_1 A_{pk}^{\pm(1)} \frac{d}{dk_2} \alpha_{pk}^{\pm} \Big|_{p_2=k_2} = \frac{s|q_f eB|}{4\sqrt{2}} \times [\Pi_k \delta_{p,k-1}(\sqrt{k} \pm \sqrt{k-1}) \mp \delta_{p,k+1}(\sqrt{k+1} \pm \sqrt{k})], \quad (\text{IV.48})$$

and eventually summing over p , using the method presented in the Appendix, we arrive, after some algebraic computations, at

$$f_{\pi^0}^{(2)} = f_{\pi^0}^{(1)}, \quad (\text{IV.49})$$

with $f_{\pi^0}^{(1)}$ given in (IV.45) for nonvanishing eB and at zero (T, μ) , and in (IV.46) for finite (T, μ, eB) . Finally, setting $i = 3$ in (IV.40), and using (IV.10) to perform the integration over k_2 and x_1 , keeping in mind that, according to (IV.33), $A_{pk}^{\pm(3)} = A_{pk}^{\pm(0)}$, we arrive easily at

$$f_{\pi^0}^{(3)} = f_{\pi^0}^{(0)}, \quad (\text{IV.50})$$

with $f_{\pi^0}^{(0)}$ given in (IV.41) for nonvanishing eB and at zero (T, μ) , and in (IV.42) for finite (T, μ, eB) . Using (IV.42) and (IV.46) as well as (IV.49) and (IV.50) for $f_{\pi^0}^{(\mu)}$, it can easily be checked that, in the limit $m_{\pi^0} \rightarrow 0$, $f_{\pi^0}^{(\mu)}$ satisfies $f_{\pi^0}^{(\mu)} = m |\mathcal{F}_{33}^{\mu\mu}|^{1/2}$, with $\mathcal{F}_{33}^{\mu\mu}$ given explicitly in [9]. Comparing this relation with the definition of $f_{\pi^0}^{(\mu)}$ from (III.31) with $\ell = 3$, it turns out that the dimensionful constant f_3 , appearing originally in the Ansatz (III.27), is, in the limit of vanishing m_{π^0} , equal to the constituent mass m . In Sec. IV B, after numerically computing $f_{\pi^0}^{(\mu)}$ from (IV.42) and (IV.46), we will determine the coefficient f_3 using (III.31) and compare its T dependence for fixed μ and eB with the T dependence of the constituent mass m for arbitrary T -dependent m_{π^0} . But, before doing this, let us analytically verify the modified GT relation (III.32). In Sec. III B, we have used (III.36) to prove (III.32). For zero magnetic fields, the explicit form of $\Upsilon_{\mu}^{\ell m}$ as a function of the fermion propagator $S(p)$ is to be used to verify (III.35). In the presence of magnetic fields, however, where nontrivial Ritus propagators $S_Q(p)$ from (II.24) are to be used to determine $\Upsilon_{\mu}^{\ell m}$, relation (III.35) cannot be directly proved. To show the GT relation for neutral magnetized pions, we use, instead, the analytical results of $\Upsilon_0^{(33)}$ and $(g_{qq\pi^0}^{(0)})^{-2}$ and verify first the following relation:

$$\Upsilon_0^{(33)}(\tilde{q}_{\pi^0}) = m m_{\pi^0} (g_{qq\pi^0}^{(0)})^{-2} + \mathcal{O}(m_{\pi^0}^2). \quad (\text{IV.51})$$

Combining further (III.27) and (III.29) for $\ell = m = 3$, and evaluating the resulting expression

$$g_{qq\pi^0} \Upsilon_{\mu}^{33}(q) = f_3 |\mathcal{F}_{33}^{00}|^{1/2} u_{\pi^0}^{(\mu)2} q_{\mu},$$

on the pion mass shell, i.e., for $q = \tilde{q}_{\pi^0} = (m_{\pi^0}, \mathbf{0})$, we obtain

$$g_{qq\pi^0} \Upsilon_0^{(33)}(\tilde{q}_{\pi^0}) = f_3 |\mathcal{F}_{33}^{00}| m_{\pi^0}, \quad (\text{IV.52})$$

which leads, together with (III.24) and (IV.51), to

$$g_{qq\pi^0} f_3 = m + \mathcal{O}(m_{\pi^0}), \quad (\text{IV.53})$$

and eventually, upon using (III.24) and (III.31), to the GT relation

$$g_{qq\pi^0}^{(\mu)} f_{\pi^0}^{(\mu)} = m + \mathcal{O}(m_{\pi^0}), \quad (\text{IV.54})$$

for neutral pions. Note that (IV.53) is the same as (III.37) with $\ell = 3$. In Sec. III B, we have shown how the GOR relation (III.33) for neutral pions,

$$m_{\pi^0}^2 f_{\pi^0}^{(\mu)2} = u_{\pi^0}^{(\mu)2} \frac{m_0 \sigma_0}{2G} + \mathcal{O}(m_0^2), \quad (\text{IV.55})$$

can be derived from (IV.53) and (III.38). As concerns the proof of (IV.51), we use (IV.34) and (IV.35) with $\mu = 0$. Using (IV.10) to perform the integration over k_3 and x_1 , we arrive at

$$\begin{aligned} \Upsilon_0^{(33)}(\tilde{q}_{\pi^0}) &= 3im m_{\pi^0} \sum_{k=0}^{\infty} \alpha_k \sum_{q_f} \int \frac{dk_0 dk_3}{(2\pi)^3} \\ &\quad \times \frac{1}{[(k_0 + m_{\pi^0})^2 - k_3^2 - 2|q_f eB|k - m^2]} \\ &\quad \times \frac{1}{[\mathbf{k}_{\parallel}^2 - 2|q_f eB| - m^2]}. \end{aligned} \quad (\text{IV.56})$$

Expanding the r.h.s. of this relation in orders of m_{π^0} , we get

$$\begin{aligned} \Upsilon_0^{(33)}(\tilde{q}_{\pi^0}) &= -3m m_{\pi^0} \sum_{k=0}^{\infty} \alpha_k \sum_{q_f} \int \frac{dk_3}{(2\pi)^2} \mathcal{S}_2^{(0)}(\omega_k) \\ &\quad + \mathcal{O}(m_{\pi^0}^2), \end{aligned} \quad (\text{IV.57})$$

at finite (T, μ, eB) . Here, $\mathcal{S}_2^{(0)}(\omega_k)$ is defined in (IV.15) and $\omega_k^2 = k_3^2 + m^2 + 2|q_f eB|k$. On the other hand, let us consider $(g_{qqM}^{(0)}(\tilde{q}_M))^{-2}$ from (IV.13). For $M = \pi^0$, it consists of two terms. Neglecting the second term proportional to $m_{\pi^0}^2$, expanding $\mathcal{S}_2^{(0)}(\omega_k^{\pi^0}(x))$, appearing in the first term around $m_{\pi^0} = 0$, and eventually integrating the resulting expression over the Feynman parameter x , we get

$$\begin{aligned} (g_{qq\pi^0}^{(0)}(\tilde{q}_{\pi^0}))^{-2} &= -3 \sum_{k=0}^{\infty} \alpha_k \sum_{q_f} \int \frac{dk_3}{(2\pi)^2} \mathcal{S}_2^{(0)}(\omega_k) \\ &\quad + \mathcal{O}(m_{\pi^0}^2), \end{aligned} \quad (\text{IV.58})$$

which, together with (IV.57), leads to (IV.51). This proves the GT and GOR relations in the limit $m_{\pi^0} \rightarrow 0$. In what follows, we will numerically verify, among others, these relations for arbitrary pion mass at finite (T, μ, eB) .

B. Numerical results

In the previous section, we determined analytically the directional neutral mesons coupling and decay constants, $g_{qqM}^{(\mu)}$, $M \in \{\sigma, \pi^0\}$ and $f_{\pi^0}^{(\mu)}$, at finite

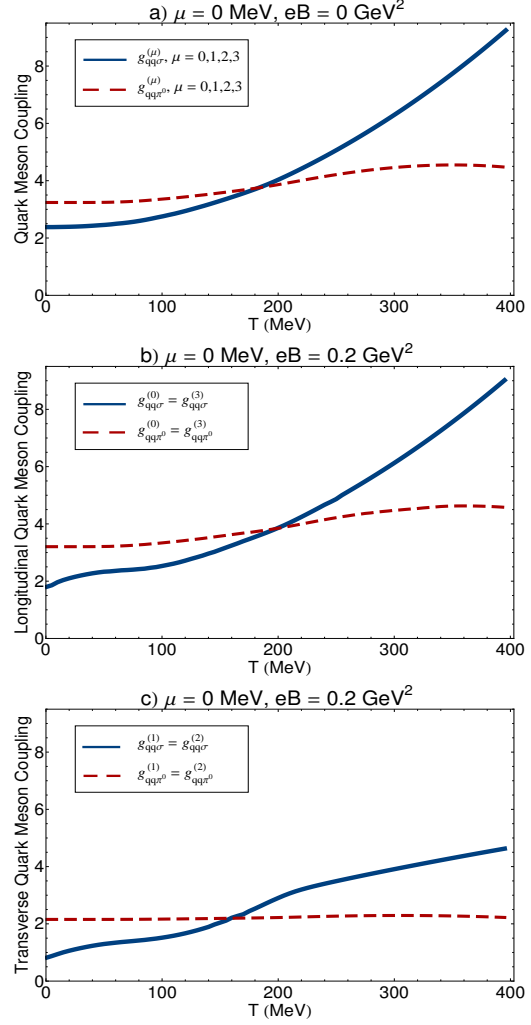


FIG. 8: The T dependence of directional quark-meson couplings is demonstrated for $eB = 0$ [panel (a)] and $eB = 0.2$ GeV² [panels (b) and (c)]. Solid blue curves are directional quark-sigma couplings $g_{qq\sigma}^{(\mu)}$, and the dashed red curves are the directional quark-pion couplings $g_{qq\pi^0}^{(\mu)}$. In contrast to $eB \neq 0$, for $eB = 0$, there is no difference between the quark-meson couplings in longitudinal and transverse directions with respect to the direction of the external magnetic field eB .

(T, μ, eB) up to an integration over k_3 momentum and a summation over discrete Landau levels. Using these analytical results, it is possible to prove the GT and GOR relations in the limit of $m_{\pi^0} \rightarrow 0$. In the present section, we will numerically determine the T dependence of $g_{qqM}^{(\mu)}$, $M \in \{\sigma, \pi^0\}$ and $f_{\pi^0}^{(\mu)}$ for zero chemical potential and finite $eB = 0.03, 0.2, 0.3$ GeV². We will compare $g_{qqM}^{(0)}$ with $g_{qqM}^{(1)}$, which corresponds to quark-meson couplings in the longitudinal and transverse directions with respect to the direction of the external magnetic field. We then present the results for the T dependence of $f_{\pi^0}^{(\mu)}$ for vanishing chemical potential and fixed eB , and will compare $f_{\pi^0}^{(0)}$ with

$f_{\pi^0}^{(1)}$. Using these numerical results, and the results from our previous paper [9], we will numerically determine the dimensionful constant f_3 , appearing in the definition (III.31) with $\ell = 3$. We will show that, for arbitrary m_{π^0} , it is given by the constituent quark mass m . Finally, a numerical verification of the GOR relation will be presented.

Let us start by fixing the parameters of our specific model, Λ, G and m_0 . As in [9, 30], we have used

$$\begin{aligned} \Lambda &= 0.6643 \text{ GeV}, & G &= 4.668 \text{ GeV}^2, \\ m_0 &= 5 \text{ MeV}. \end{aligned} \quad (\text{IV.59})$$

The UV momentum cutoff Λ is necessary to perform the k_3 integrations in the results for $g_{qqM}^{(\mu)}$, $M \in \{\sigma, \pi^0\}$ and $f_{\pi^0}^{(\mu)}$ from previous sections. It is also used to determine the upper limit c for the summation over Landau levels. We will fix c by building the ratio $\lfloor \frac{\Lambda^2}{|q_f eB|} \rfloor \equiv c$, where $\lfloor z \rfloor$ is the greatest integer less than or equal to z . To perform the momentum integrations over \mathbf{k} and k_3 , we use, as in [9, 30], smooth cutoff

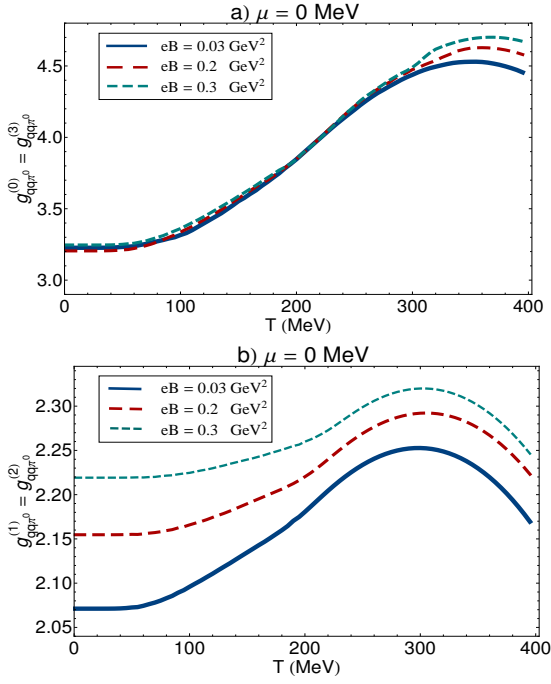


FIG. 9: The T dependence of directional quark-pion couplings $g_{qq\pi^0}^{(\mu)}$ are demonstrated for vanishing chemical potential and $eB = 0.03, 0.2, 0.3 \text{ GeV}^2$. In panels (a) and (b), the longitudinal coupling $g_{qq\pi^0}^{(0)} = g_{qq\pi^0}^{(3)}$ and transverse coupling $g_{qq\pi^0}^{(1)} = g_{qq\pi^0}^{(2)}$ are plotted, respectively. The couplings show different behaviors by increasing the strength of the magnetic field eB at fixed T , and similar behaviors before and after the transition temperature $T_c \sim 200 \text{ MeV}$.

functions

$$\begin{aligned} f_{\Lambda,0} &= \frac{1}{1 + \exp\left(\frac{|\mathbf{k}| - \Lambda}{A}\right)}, \\ f_{\Lambda,B}^k &= \frac{1}{1 + \exp\left(\frac{\sqrt{k_3^2 + 2|q_f eB|k} - \Lambda}{A}\right)}, \end{aligned} \quad (\text{IV.60})$$

which correspond to integrals with vanishing and non-vanishing magnetic fields. In $f_{\Lambda,B}^k$, the upper index k labels the Landau levels. In (IV.60), A is a free parameter, that determines the sharpness of the cutoff. It is fixed to be $A = 0.05\Lambda$, with Λ from (IV.59). As we have also mentioned in Sec. II, fixing the free param-

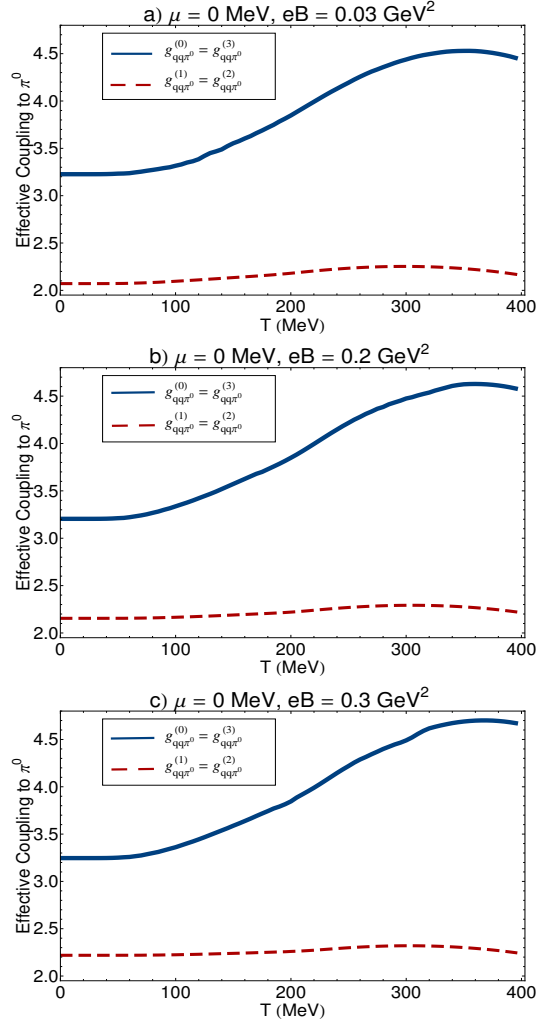


FIG. 10: Longitudinal (blue solid curves) and transverse (red dashed curves) quark-pion couplings, $g_{qq\pi^0}^{(0)} = g_{qq\pi^0}^{(3)}$ and $g_{qq\pi^0}^{(1)} = g_{qq\pi^0}^{(2)}$, are compared in the interval $T \in [0, 400] \text{ MeV}$ for vanishing chemical potential and various $eB = 0.03 \text{ GeV}^2$ [panel (a)], $eB = 0.2 \text{ GeV}^2$ [panel (b)] and $eB = 0.3 \text{ GeV}^2$ [panel (c)]. As it turns out, the longitudinal coupling is always greater than the transverse coupling.

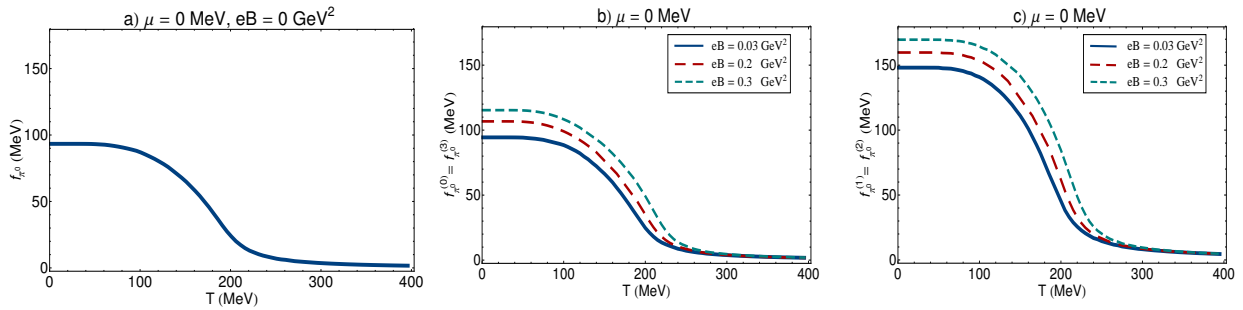


FIG. 11: [Panel (a)] The T dependence of f_{π_0} for vanishing chemical potential and magnetic field. Panels (b) and (c): The T dependence of longitudinal [panel (b)] and transverse [panel (c)] decay constants of neutral pions are plotted for zero chemical potential and nonvanishing $eB = 0.03, 0.2, 0.3 \text{ GeV}^2$.

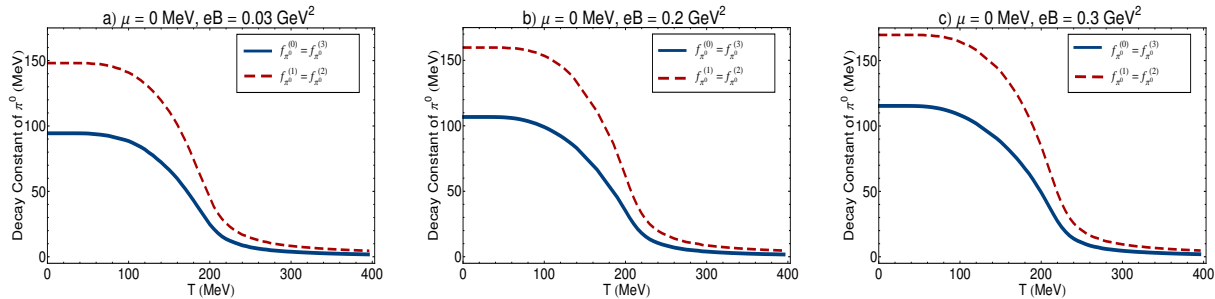


FIG. 12: The T dependence of longitudinal (blue solid curves) and transverse (red dashed curves) decay constants of neutral pions, $f_{\pi_0}^{(0)}$ and $f_{\pi_0}^{(1)}$, are compared for vanishing chemical potential and nonvanishing $eB = 0.03, 0.2, 0.3 \text{ GeV}^2$. As it turns out, $f_{\pi_0}^{(0)} < f_{\pi_0}^{(1)}$.

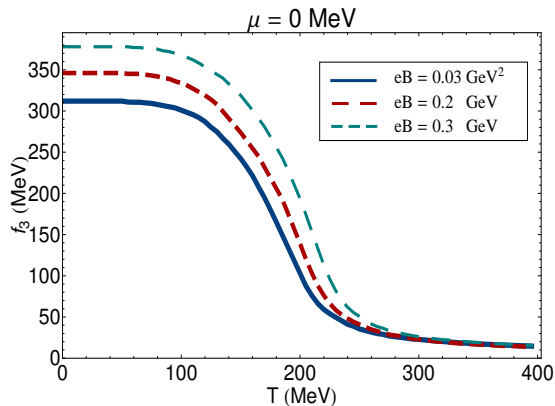


FIG. 13: The T dependence of f_3 appearing in the PCAC relation (III.27). Here, f_3 is determined using $f_3 = f_{\pi_0}^{(0)} |\mathcal{F}_{33}^{00}|^{-1/2}$ from (III.31) with $\ell = 3$. Comparing these results with the corresponding data from the T dependence of the constituent quark mass m , it turns out that $f_3 = m$ for an arbitrary value of m_{π^0} .

eters of the model as in (IV.59), the constituent mass m at zero (T, μ, eB) turns out to be $m \sim 308 \text{ MeV}$, as expected. Moreover, the pion mass and decay constant for vanishing (T, μ, eB) are given by $m_{\pi} \sim 139.6 \text{ MeV}$ and $f_{\pi} = 93.35 \text{ MeV}$, respectively. These values are expected from the phenomenology of a two-flavor

NJL model [3]. We will limit all our numerical computations in this section in the interval $T \in [0, 400] \text{ MeV}$ for vanishing μ and $eB = 0, 0.03, 0.2, 0.3 \text{ GeV}^2$. As we have shown in [9, 30], in this interval the chiral symmetry of the theory is broken and the quark condensate $\sigma_0 \sim \langle \bar{\psi}\psi \rangle$, appearing in $m = m_0 + \sigma_0$, plays the role of the order parameter of the transition from a chirally broken to a chirally symmetric phase.

In Figs. 8(a)-(c), we have plotted the T dependence of the directional quark-meson coupling $g_{qq\sigma}^{(\mu)}$ (solid blue curves) and $g_{qq\pi^0}^{(\mu)}$ (red dashed curves) for $eB = 0$ [Fig. 8(a)] and $eB = 0.2 \text{ GeV}^2$ [Figs. 8(b) and 8(c)]. Whereas for $eB = 0$, there is no difference between $g_{qqM}^{(\mu)}$, $M \in \{\sigma, \pi^0\}$ for different directions $\mu = 0, \dots, 3$, for $eB \neq 0$, the longitudinal and transverse quark-meson couplings for σ and π^0 are different [compare the solid blue and dashed red curves in Figs. 8(b) and 8(c)]. At certain temperature T_{cross} , the two curves cross, i.e., $g_{qq\sigma}^{(\mu)}$ becomes equal to $g_{qq\pi^0}^{(\mu)}$. For $T < T_{\text{cross}}$, $g_{qq\sigma}^{(\mu)} < g_{qq\pi^0}^{(\mu)}$ and for $T > T_{\text{cross}}$, $g_{qq\sigma}^{(\mu)} > g_{qq\pi^0}^{(\mu)}$. Moreover, as it turns out, for $eB = 0$, $T_{\text{diss.}} < T_{\text{cross}} < T_{\text{Mott}}$. For $eB \neq 0$, however, we have to separate the longitudinal and transverse cases. Whereas for longitudinal couplings, we have $T_{\text{diss.}} < T_{\text{cross}} < T_{\text{Mott}}$, for transverse couplings, we get $T_{\text{cross}} < T_{\text{diss.}} < T_{\text{Mott}}$. Whether this tem-

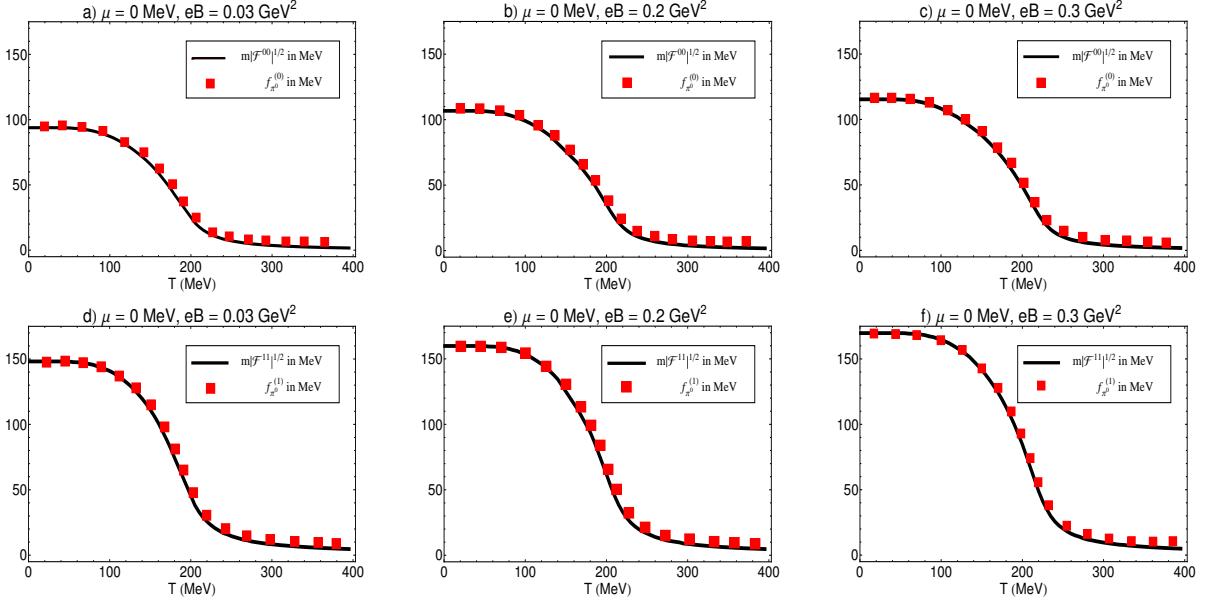


FIG. 14: The T dependence of $f_{\pi_0}^{(\mu)}$ (red squares) is compared with the T dependence of $m|\mathcal{F}_{33}^{\mu\mu}|^{1/2}$ (black solid lines) for longitudinal $\mu = 0, 3$ [panels (a)-(c)] and transverse directions $\mu = 1, 2$ [panels (d)-(e)]. Together with the definition $f_{\pi_0}^{(\mu)} = f_3|\mathcal{F}_{33}^{\mu\mu}|^{1/2}$ from (III.31) with $\ell = 3$, we obtain $f_3 = m$, as expected also from the comparison of the data of f_3 in Fig. 13 and the constituent quark mass $m = m_0 + \sigma_0$ in Fig. 1.

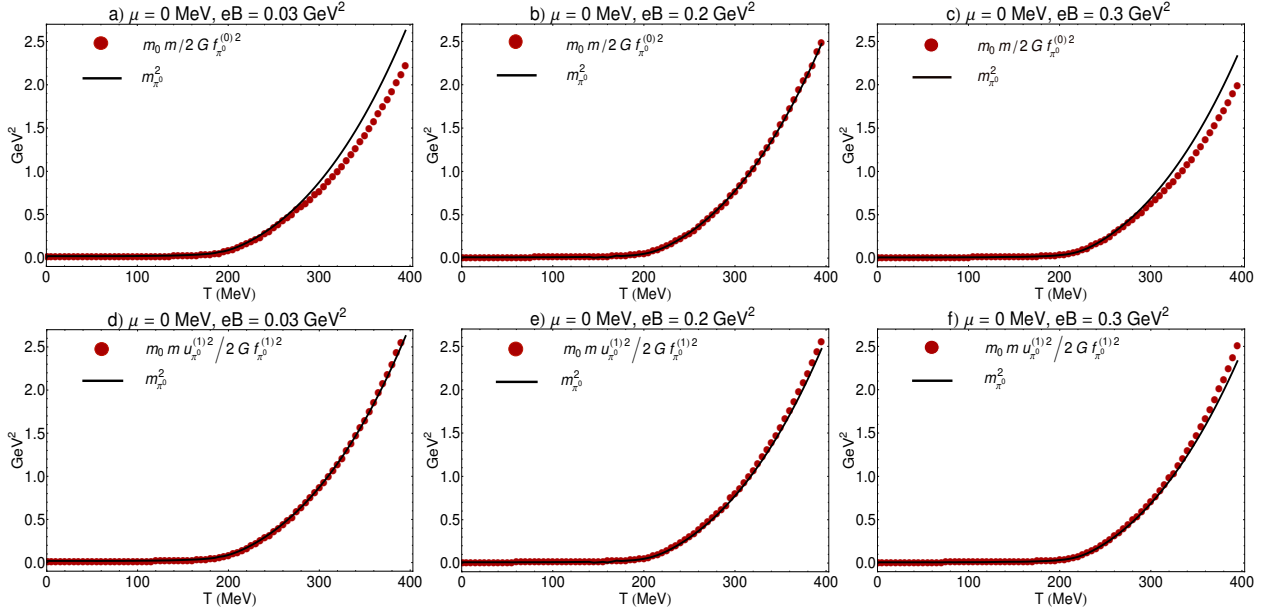


FIG. 15: To verify the relation (IV.61), suggested by the GOR relation (IV.55), the T dependence of $m_{\pi_0}^2$ (black solid lines) is compared with $\frac{m_0 m}{2G f_{\pi_0}^{(0)2}}$ (red dots) [panels (a)-(c)] and with $u_{\pi_0}^{(1)2} \frac{m_0 m}{2G f_{\pi_0}^{(1)2}}$ (red dots) [panels (d)-(f)]. Relation (IV.61) seems to be exact, especially at temperatures below the critical temperature and for small eB .

perature is of certain relevance, in particular, in the scattering length and the total cross section of meson-meson scattering, where the thermodynamic properties of quark-meson couplings play an important role is under investigation.

In Fig. 9, the T dependence of directional quark-

pion couplings, $g_{qq\pi_0}^{(\mu)}$, is plotted for vanishing chemical potential and various $eB = 0, 0.03, 0.2, 0.3 \text{ GeV}^2$. The longitudinal quark-pion coupling $g_{qq\pi_0}^{(0)} = g_{qq\pi_0}^{(3)}$ from (IV.13) with $M = \pi^0$ is plotted in Fig. 9(a), and the transverse quark-pion coupling $g_{qq\pi_0}^{(1)} = g_{qq\pi_0}^{(2)}$ from (IV.25) with $M = \pi^0$ is plotted in Fig. 9(b). Whereas

the behavior of longitudinal and transverse couplings is different by increasing the strength of the external magnetic field for a fixed temperature, it turns out to be similar when we increase the temperature from $T = 0$ to $T = 400$ MeV. An inflection point arises in directional quark-pion coupling constants around the critical temperature $T \sim 200$ MeV. Comparing the longitudinal and transverse quark-pion couplings in Fig. 10, it turns out that $g_{qq\pi^0}^{(0)} > g_{qq\pi^0}^{(1)}$ in the interval $T \in [0, 400]$ MeV and for fixed chemical potential and magnetic fields. This is a direct consequence of the fact that the transverse refraction index of pions is larger than unity: As we have seen in Fig. 4, $u_{\pi^0}^{(1)} = u_{\pi^0}^{(2)} > 1$. Using $g_{qq\pi^0}^{(\mu)} = g_{qq\pi^0} |\mathcal{F}_{33}^{\mu\mu}|^{-1/2}$ from (III.24) with $\ell = 3$, and $u_{\pi^0}^{(\mu)} = |\mathcal{F}_{33}^{\mu\mu}/\mathcal{F}_{33}^{00}|^{1/2}$ from (III.17), we will get $g_{qq\pi^0}^{(0)} = g_{qq\pi^0} |\mathcal{F}_{33}^{00}|^{-1/2}$ as well as $g_{qq\pi^0}^{(1)} = g_{qq\pi^0}^{(0)}/u_{\pi^0}^{(1)}$. For $u_{\pi^0}^{(1)} > 1$, it turns out that $g_{qq\pi^0}^{(0)} > g_{qq\pi^0}^{(1)}$, as is observed in Fig. 10.

Let us now consider the longitudinal and transverse pion decay constants, $f_{\pi^0}^{(0)} = f_{\pi^0}^{(3)}$ and $f_{\pi^0}^{(1)} = f_{\pi^0}^{(2)}$ from (IV.42) and (IV.46), respectively. In Fig. 11(a), the T dependence of f_{π^0} is plotted for vanishing chemical potential and magnetic fields. In Figs. 11(b) and 11(c), the T dependence of longitudinal and transverse decay constants of neutral pions, $f_{\pi^0}^{(0)}$ and $f_{\pi^0}^{(1)}$, is plotted for zero chemical potential and nonvanishing magnetic fields $eB = 0.03, 0.2, 0.3$ GeV². In both cases, $f_{\pi^0}^{(\mu)}$ is large below the critical temperature and decreases with increasing temperature. At a fixed temperature, the directional pion decay constants increase as the strength of the magnetic field increases. In Figs. 12(a)-12(c), we have compared the T dependence of the longitudinal and transverse decay constants for $\mu = 0$ and $eB = 0.03, 0.2, 0.3$ GeV². As it turns out, $f_{\pi^0}^{(0)} < f_{\pi^0}^{(1)}$. This behavior is again related to $u_{\pi^0}^{(1)} > 1$ from Fig. 4: Using the definition $f_{\pi^0}^{(\mu)} = f_3 |\mathcal{F}_{33}^{\mu\mu}|^{1/2}$ from (III.31) with $\ell = 3$, and $u_{\pi^0}^{(\mu)} = |\mathcal{F}_{33}^{\mu\mu}/\mathcal{F}_{33}^{00}|^{1/2}$ from (III.17), it turns out that $f_{\pi^0}^{(0)} = f_3 |\mathcal{F}_{33}^{00}|^{1/2}$ and $f_{\pi^0}^{(1)} = f_{\pi^0}^{(0)} u_{\pi^0}^{(1)}$. For $u_{\pi^0}^{(1)} > 1$, we have therefore $f_{\pi^0}^{(0)} < f_{\pi^0}^{(1)}$, as observed in Fig. 12. Note that combining $g_{qq\pi^0}^{(1)} = g_{qq\pi^0}^{(0)}/u_{\pi^0}^{(1)}$ and $f_{\pi^0}^{(1)} = f_{\pi^0}^{(0)} u_{\pi^0}^{(1)}$ yields the GT relation (III.32).

Using the corresponding data of $f_{\pi^0}^{(\mu)}$ and the definition of directional decay constant $f_{\pi^0}^{(\mu)}$ from (III.31) with $\ell = 3$, it is possible to determine the T dependence of f_3 defined by $f_{\pi^0}^{(\mu)} = f_3 |\mathcal{F}_{33}^{\mu\mu}|^{1/2}$. To do this, we have also used the data corresponding to the T dependence of $\mathcal{F}_{33}^{\mu\mu}$ from our previous paper [9]. In Fig. 13, we have presented the T dependence of f_3 for vanishing chemical potential and various $eB = 0.03, 0.2, 0.3$ GeV². Comparing these results with the corresponding data from the T dependence of the constituent quark mass m , it turns out that

$f_3 = m$ for an arbitrary value of m_{π^0} . According to our arguments from [9], for a fixed T and μ , the constituent quark mass increases with increasing strength of the magnetic field (see also Fig. 1). This is because of the phenomenon of magnetic catalysis [5, 6]. We conclude therefore that the behavior of longitudinal and transverse pion decay constants in external magnetic fields at fixed temperature and chemical potential is mainly affected by this phenomenon.

Note that another way to verify $f_3 = m$ is to compare the T dependence of $f_{\pi^0}^{(\mu)}$ on the l.h.s. of the relation $f_{\pi^0}^{(\mu)} = m |\mathcal{F}_{33}^{\mu\mu}|^{1/2}$ with the T dependence of $m |\mathcal{F}_{33}^{\mu\mu}|^{1/2}$ on the r.h.s. of this relation for longitudinal directions $\mu = 0, 3$ [Figs. 14(a)-14(c)], and transverse directions $\mu = 1, 2$ [Figs. 14(d)-14(f)]. The red squares denote the data for $f_{\pi^0}^{(\mu)}$, $\mu = 0, 1$ and the black solid lines the combination $m |\mathcal{F}_{33}^{00}|^{1/2}$ for longitudinal $\mu = 0, 3$ and $m |\mathcal{F}_{33}^{11}|^{1/2}$ for transverse $\mu = 1, 2$ directions.

Let us now consider the GOR relation (IV.55) for neutral pions. In Sec. IV A, we have analytically proved the GOR relation (IV.55) in the limit of vanishing m_{π^0} . In Fig. 15, however, we have compared the T dependence of the expression $u_{\pi^0}^{(\mu)2} \frac{m_0 m}{2G f_{\pi^0}^{(\mu)}}$ (red dots) with the T dependence of $m_{\pi^0}^2$ (black solid lines) for any value of m_{π^0} for various $eB = 0.03, 0.2, 0.3$ GeV². In Figs. 15(a)-15(c), we present the data for longitudinal directions, i.e. for $\mu = 0$ with $u_{\pi^0}^{(0)} = u_{\pi^0}^{(3)} = 1$ [see Fig. 4(b) for the longitudinal refraction index of neutral pions], and in Figs 15(d)-15(f) the data for transverse directions are presented. Note that, according to Fig. 4 [9], the transverse refraction index of neutral pions is larger than unity. As it is shown in Fig. 15, the relation

$$m_{\pi^0}^2 = u_{\pi^0}^{(\mu)2} \frac{m_0 m}{2G f_{\pi^0}^{(\mu)}}, \quad (\text{IV.61})$$

seems to be exact in the interval below the critical temperature. As we have explained in [9], the critical temperature is defined by the temperature from which the neutral pion mass starts to increase. The deviations of the expression on the r.h.s. of (IV.61) from $m_{\pi^0}^2$ on the l.h.s. of this relation depend on eB and T .

V. SUMMARY AND CONCLUSIONS

Uniform magnetic fields affect the properties of mesons in a hot and dense quark matter. In our previous paper [9], we systematically studied these effects on the pole and screening mass as well as the refraction index of pions. In the present paper, we continued with exploring the effect of constant magnetic fields on the pion weak decay constant. One of our first observations was that external magnetic fields break the

isospin symmetry of pions, insofar as charged and neutral pions behave differently in the external magnetic fields. In contrast to the studies performed in [32, 33], where chiral perturbation theory is used to study the effect of constant magnetic fields on the properties of charged pions, we focused on the properties of neutral pions in external magnetic fields.

In this paper, following the same method as in our previous paper [9], we used an appropriate derivative expansion up to second order and derived the effective action of a two-flavor bosonized NJL model at finite (T, μ, eB) in this approximation. The resulting effective action is given as a functional of σ and π^0 mesons and includes a kinetic and a potential part. To derive the mass and refraction indices of neutral mesons, we focused, in particular, on the nontrivial kinetic part of the effective action, including nontrivial form factors. They were evaluated in [9] using the method presented in Sec. II. As it turns out, they play an essential role in defining the pole and screening mass as well as the directional refraction indices of neutral pions. As concerns the pions' refraction index, it turns out that in the presence of a constant magnetic field, aligned in a fixed direction, the refraction indices of neutral pions parallel to the direction of the external magnetic field and in the plane perpendicular to this direction are different. Within our approximation, where the contributions of pion-pion interactions are neglected, and at $T \neq 0$ and $eB \neq 0$, the longitudinal refraction index is unity for all nonvanishing T and eB , while the transverse refraction index is larger than unity. This is in contrast to the case $T = 0$ and $eB = 0$, where the refraction index for neutral pions in all spatial directions is equal to unity. This is also in contrast to the case $T \neq 0$ and $eB = 0$, where all spatial refraction indices are equal to and smaller than unity [14–16]. One of the possibilities to improve the results in this paper is to include pion self-interaction terms in the original Lagrangian for pions and to study the T dependence of directional refraction indices in the longitudinal and transverse directions in that setup.

Our central analytical result in this paper is presented in Sec. III. In Sec. III A, we briefly reviewed the method introduced in [3] and derived the weak decay constant of pions at zero T and eB . In this case, the pions satisfy an ordinary isotropic energy dispersion relation $E_\pi^2 = \mathbf{q}^2 + m_\pi^2$, and the weak decay constant f_π is given by combining the ordinary PCAC relation and the Feynman integral corresponding to a one-pion-to-vacuum amplitude. As a by-product, the momentum-dependent quark-pion coupling constant $g_{qq\pi}(q)$ is also defined. Our starting point in Sec. III B, however, was an anisotropic energy dispersion relation, $E_\pi^2 = u_\pi^{(i)2} q_i^2 + m_\pi^2$, including directional refraction indices $u_\pi^{(i)}$, $i = 1, 2, 3$. Note that, according to the above arguments, the case of nonvanishing magnetic field and/or finite temperature can be viewed only as special cases of the general assumption

of Sec. III B.¹² Introducing a modified PCAC relation with nontrivial four-vector $u_{\pi_a}^{(\mu)} = (1, u_{\pi_a}^{(i)})$, as given in (III.27), and following the same arguments as in Sec. III A, we derived the modified GT and GOR relations, (III.32) and (III.33), including the directional pion weak decay constant $f_{\pi^0}^{(\mu)}$ and the directional quark-pion coupling constant $g_{qq\pi^0}^{(\mu)}$.

In Sec. IV, we then used the results arising from the general treatment presented in Sec. III B and determined $g_{qq\pi^0}^{(\mu)}$ as well as $f_{\pi^0}^{(\mu)}$ at finite T and eB first analytically in Sec. IV A, and then numerically in Sec. IV B. As it turns out, the longitudinal and transverse quark-pion coupling and weak decay constants satisfy $g_{qq\pi^0}^{(0)} = g_{qq\pi^0}^{(3)} \neq g_{qq\pi^0}^{(1)} = g_{qq\pi^0}^{(2)}$ and $f_{\pi^0}^{(0)} = f_{\pi^0}^{(3)} \neq f_{\pi^0}^{(1)} = f_{\pi^0}^{(2)}$. We determined numerically their T dependence for various eB . We showed that, whereas $g_{qq\pi^0}^{(0)} > g_{qq\pi^0}^{(1)}$, we have $f_{\pi^0}^{(0)} < f_{\pi^0}^{(1)}$. This is a direct consequence of the fact that $1 = u_{\pi^0}^{(0)} < u_{\pi^0}^{(1)}$, as it is shown in Fig. 4. Moreover, for a fixed μ and eB , whereas the mass of neutral pions increases with increasing T [see Fig. 3(b)], the directional decay constants of pions decrease with T . At fixed μ and T , they increase with increasing strength of the external magnetic field (see Fig. 11). As concerns the behavior of pions, directional decay constants $f_{\pi^0}^{(\mu)}$, $\mu = 0, \dots, 3$ near the chiral transition point T_c , it turns out, that, independent of the direction, they are almost constant but large at $T \ll T_c$, start to decrease at $T \simeq T_c$ and remain constant but very small at $T \gg T_c$. Moreover, the slope of this decrease as a function of T depends on the strength of the external magnetic field. The behavior of $g_{qq\pi^0}^{(\mu)}$ and $f_{\pi^0}^{(\mu)}$ in the external magnetic field and at finite T is strongly related to the behavior of the constituent quark mass m at finite T and eB . This relationship is reflected in the low energy relations of neutral pions, the GT and GOR relations. We not only derived these relations analytically in Sec. IV A, but also verified them numerically in Sec. IV B. The behavior of the constituent quark mass m at finite T and eB was discussed extensively in our previous paper [9]. Comparing Figs. 1 and 11(a)-11(c), it turns out that m and $f_{\pi^0}^{(\mu)}$ have similar T dependence for a fixed eB . The phenomenon of magnetic catalysis is reflected in the fact that at fixed μ and T , they both increase with increasing eB . As we have shown in Sec. III, $f_{\pi^0}^{(\mu)}$ and m are proportional, and the proportionality factor is, according to the GT relation (III.32), $1/g_{qq\pi^0}^{(\mu)}$. Let us finally note that our results can be improved by improving the approximation we have

¹² Remember that at finite temperature, the refraction indices satisfy $u_\pi^{(1)} = u_\pi^{(2)} = u_\pi^{(3)} = u$ [see (I.4)]. In the nonvanishing magnetic field, however, they satisfy $u_\pi^{(1)} = u_\pi^{(2)} \neq u_\pi^{(3)}$ [see (I.5)].

used to determine the kinetic coefficients to higher order derivative expansion, or by making use of the functional renormalization group method, which was recently used in [34].

Appendix: Useful relations

In this appendix, we present a number of useful relations leading to the analytical results presented in Sec. IV. Let us start with the orthonormality relations of $f_p^{\pm s}$ appearing in (II.26),

$$\begin{aligned}
& \int dx_1 f_p^{+s}(x) f_k^{+s}(x) \Big|_{p_2=k_2} = \delta_{pk}, \\
& \int dx_1 x_1 f_p^{+s}(x) f_k^{+s}(x) \Big|_{p_2=k_2} = \ell_B \left\{ \Pi_k C_k \delta_{p,k-1} \right. \\
& \quad \left. + \Pi_{k+1} C_{k+1} \delta_{p,k+1} + s \ell_B k_2 \delta_{p,k} \right\}, \\
& \int dx_1 x_1^2 f_p^{+s}(x) f_k^{+s}(x) \Big|_{p_2=k_2} \\
& = \ell_B^2 \left\{ (2C_{2k+1}^2 + \ell_B^2 k_2^2) \delta_{pk} + \Pi_k \Pi_{k-1} C_k C_{k-1} \delta_{p,k-2} \right. \\
& \quad \left. + C_{k+1} C_{k+2} \delta_{p,k+2} + 2\Pi_k C_k s \ell_B k_2 \delta_{p,k-1} \right. \\
& \quad \left. + 2\Pi_{k+1} C_{k+1} s \ell_B k_2 \delta_{p,k+1} \right\}, \tag{A.1}
\end{aligned}$$

and

$$\begin{aligned}
& \int dk_2 f_p^{+s}(0) f_k^{+s}(0) \Big|_{p_2=k_2} = \frac{\delta_{pk}}{\ell_B^2}, \\
& \int dk_2 k_2 f_p^{+s}(0) f_k^{+s}(0) \Big|_{p_2=k_2} = -\frac{s}{\ell_B^3} \left\{ C_{k+1} \delta_{p,k+1} \right. \\
& \quad \left. + \Pi_k C_k \delta_{p,k-1} \right\}, \\
& \int dk_2 k_2^2 f_p^{+s}(0) f_k^{+s}(0) \Big|_{p_2=k_2} = \frac{1}{\ell_B^4} \left\{ 2C_{2k+1}^2 \delta_{pk} \right. \\
& \quad \left. + \Pi_k \Pi_{k-1} C_k C_{k-1} \delta_{p,k-2} + C_{k+1} C_{k+2} \delta_{p,k+2} \right\}. \tag{A.2}
\end{aligned}$$

Here, $C_k \equiv \sqrt{\frac{k}{2}}$ and $\ell_B \equiv \frac{1}{\sqrt{|q_f e B|}}$. To derive these relations, we have used

$$\begin{aligned}
x_1 f_p^{+s}(x) & = \ell_B \left\{ \Pi_{p+1} C_{p+1} f_{p+1}^{+s}(x) + \Pi_p C_p f_{p-1}^{+s}(x) \right. \\
& \quad \left. + s \ell_B p_2 f_p^{+s}(x) \right\}, \\
p_2 f_p^{+s}(x) & = -\frac{s}{\ell_B} \left\{ \Pi_{p+1} C_{p+1} f_{p+1}^{+s}(x) \right. \\
& \quad \left. + \Pi_p C_p f_{p-1}^{+s}(x) \right\}. \tag{A.3}
\end{aligned}$$

Apart from (IV.44), we have

$$\begin{aligned}
& \int dx_1 dk_2 x_1 A_{pk}^{+(1)} \alpha_{pk}^+ = \frac{1}{4\ell_B} \left\{ 2\Pi_k C_k \alpha_k \right. \\
& \quad \left. - \Pi_k \delta_{p,k-1} (C_k + C_{k-1}) \right. \\
& \quad \left. - \Pi_{k+1} \delta_{p,k+1} (C_{k+1} - C_k) \right\}, \tag{A.4}
\end{aligned}$$

as well as

$$\begin{aligned}
& \int dx_1 dk_2 x_1 A_{pk}^{-(1)} \alpha_{pk}^- \\
& = -\frac{1}{4\ell_B} \left\{ \Pi_k \delta_{p,k-1} (C_k - C_{k-1}) \right. \\
& \quad \left. - \Pi_{k+1} \delta_{p,k+1} (C_{k+1} - C_k) \right\}, \tag{A.5}
\end{aligned}$$

which can be used to derive (IV.48) as well as

$$\begin{aligned}
& \int dx_1 dk_2 \frac{d}{dk_2} \left[\alpha_{pk}^+ A_{pk}^{+(1)} + \alpha_{pk}^- A_{pk}^{-(1)} \right] \Big|_{p_2=k_2} \\
& = -\frac{s}{2\ell_B^2} [\Pi_k \delta_{p,k-1} + \delta_{p,k-1}]. \tag{A.6}
\end{aligned}$$

Similarly, we have

$$\begin{aligned}
& \int dx_1 dk_2 \frac{d}{dk_2} \left[\alpha_{pk}^+ A_{pk}^{+(0)} + \alpha_{pk}^- A_{pk}^{-(0)} \right] \Big|_{p_2=k_2} \\
& = -\frac{s}{2\ell_B^2} [\Pi_k \delta_{p,k-1} + \delta_{p,k-1}]. \tag{A.7}
\end{aligned}$$

Finally, we present the method leading to $g_{qq\pi^0}^{(1)}$ from (IV.25) and to $f_{\pi^0}^{(1)}$ from (IV.45). The relations leading to (IV.25) and (IV.49) have the following general structure:

$$\begin{aligned}
I & \equiv \sum_{p,k=0}^{\infty} \int_0^1 dx f(p, k, x) \\
& \quad \times [\Pi_k \delta_{p,k-1} F(p, k) + \delta_{p,k+1} G(p, k)]. \tag{A.8}
\end{aligned}$$

The aim is to show

$$I = \sum_{k=0}^{\infty} \int_0^1 dx f(k+1, k, x) [F(k, k) + G(k+1, k)]. \tag{A.9}$$

Starting from (A.8) and summing over p , we arrive first at

$$\begin{aligned}
I & = \sum_{k=0}^{\infty} \int_0^1 dx [\Pi_k f(k-1, k, x) F(k-1, k) \\
& \quad + f(k+1, k, x) G(k+1, k)]. \tag{A.10}
\end{aligned}$$

Changing the variables in the first term and using the property of $f(p, k, x)$

$$f(k, k+1, x) = f(k, k+1, 1-x),$$

we arrive at

$$I = \sum_{k=0}^{\infty} \int_0^1 dx [f(k, k+1, 1-x)F(k) + f(k+1, k, x)G(k+1)].$$

Then using the symmetry property

$$\int_0^1 dx f(k+1, k, 1-x) = \int_0^1 dx f(k+1, k, x),$$

we arrive at (A.9). In all our examples in Sec. IV, $f(p, k, x)$ has the general form

$$f(p, k, x) = \frac{A + B\sqrt{pk}}{[C + x(1-x)m^2 + D(px + k(1-x))]^2}.$$

-
- [1] J. W. Holt, N. Kaiser and W. Weise, *Nuclear chiral dynamics and thermodynamics*, arXiv:1304.6350 [nucl-th].
- [2] S. -i. Nam and H. -C. Kim, *Pion weak decay constant at finite density from the instanton vacuum*, Phys. Lett. B **666**, 324 (2008), arXiv:0805.0060 [hep-ph].
- [3] M. Buballa, *NJL model analysis of quark matter at large density*, Phys. Rept. **407**, 205 (2005), arXiv:hep-ph/0402234.
- [4] T. Hell, S. Rossner, M. Cristoforetti and W. Weise, *Thermodynamics of a three-flavor nonlocal Polyakov-Nambu-Jona-Lasinio model*, Phys. Rev. D **81**, 074034 (2010), arXiv:0911.3510 [hep-ph].
- [5] K. G. Klimenko, *Three-dimensional Gross-Neveu model at nonzero temperature and in an external magnetic field*, Z. Phys. C **54**, 323 (1992).
- [6] V. P. Gusynin, V. A. Miransky, I. A. Shovkovy, *Dimensional reduction and catalysis of dynamical symmetry breaking by a magnetic field*, Nucl. Phys. B **462**, 249 (1996), arXiv:hep-ph/9509320.
- [7] D. E. Kharzeev, K. Landsteiner, A. Schmitt and H. -U. Yee, “*Strongly interacting matter in magnetic fields*”: an overview, Lect. Notes Phys. **871**, 1 (2013), arXiv:1211.6245 [hep-ph].
- [8] R. Gatto and M. Ruggieri, *Quark matter in a strong magnetic background*, Lect. Notes Phys. **871**, 87 (2013), arXiv:1207.3190 [hep-ph].
- I. A. Shovkovy, *Magnetic catalysis: A review*, Lect. Notes Phys. **871**, 13 (2013), arXiv:1207.5081 [hep-ph].
- F. Preis, A. Rebhan and A. Schmitt, *Inverse magnetic catalysis in field theory and gauge-gravity duality*, Lect. Notes Phys. **871**, 51 (2013), arXiv:1208.0536 [hep-ph].
- E. J. Ferrer and V. de la Incera, *Magnetism in dense quark matter*, Lect. Notes Phys. **871**, 399 (2013), arXiv:1208.5179 [nucl-th].
- E. S. Fraga, *Thermal chiral and deconfining transitions in the presence of a magnetic background*, Lect. Notes Phys. **871**, 121 (2013), arXiv:1208.0917 [hep-ph].
- K. Fukushima, *Views of the chiral magnetic effect*, Lect. Notes Phys. **871**, 241 (2013), arXiv:1209.5064 [hep-ph].
- M. A. Andreichikov, B. O. Kerbikov, V. D. Orlovsky and Y. A. Simonov, *Meson spectrum in strong magnetic fields*, Phys. Rev. D **87**, 094029 (2013), arXiv:1304.2533 [hep-ph].
- A. Ayala, L. A. Hernandez, J. Lopez, A. J. Mizher, J. C. Rojas and C. Villavicencio, *Phase diagram for charged scalars in a magnetic field at finite temperature*, arXiv:1305.1583 [hep-ph].
- C. S. Machado, F. S. Navarra, E. G. de Oliveira, J. Noronha and M. Strickland, *Heavy quarkonium production in a strong magnetic field*, Phys. Rev. D **88**, 034009 (2013), arXiv:1305.3308 [hep-ph].
- [9] S. Fayazbakhsh, S. Sadeghian and N. Sadooghi, *Properties of neutral mesons in a hot and magnetized quark matter*, Phys. Rev. D **86**, 085042 (2012), arXiv:1206.6051 [hep-ph].
- [10] N. O. Agasian and I. A. Shushpanov, *Gell-Mann-Oakes-Renner relation in a magnetic field at finite temperature*, JHEP **0110**, 006 (2001), arXiv:hep-ph/0107128.
- [11] I. V. Selyuzhenkov [STAR Collaboration], *Global polarization and parity violation study in Au + Au collisions*, Rom. Rep. Phys. **58**, 049 (2006), arXiv:nucl-ex/0510069.
- D. E. Kharzeev, L. D. McLerran and H. J. Warringa, *The effects of topological charge change in heavy ion collisions: ‘Event by event P and CP violation’*, Nucl. Phys. A **803**, 227 (2008), arXiv:0711.0950 [hep-ph].
- A. Bzdak and V. Skokov, *Event-by-event fluctuations of magnetic and electric fields in heavy ion collisions*, Phys. Lett. B **710**, 171 (2012), arXiv:1111.1949 [hep-ph].
- [12] V. Skokov, A. Y. Illarionov and V. Toneev, *Estimate of the magnetic field strength in heavy-ion collisions*, Int. J. Mod. Phys. A **24**, 5925 (2009), arXiv:0907.1396 [nucl-th].
- K. Tuchin, *Time and space dependence of electromagnetic field in relativistic heavy-ion collisions*, Phys. Rev. C **88**, 024911 (2013), arXiv:1305.5806 [hep-ph].
- [13] E. V. Shuryak, *Physics of the pion liquid*, Phys. Rev. D **42**, 1764 (1990).
- [14] D. T. Son and M. A. Stephanov, *Pion propagation near the QCD chiral phase transition*, Phys. Rev. Lett. **88**, 202302 (2002), arXiv:hep-ph/0111100.
- D. T. Son and M. A. Stephanov, *Real time pion propagation in finite temperature QCD*, Phys. Rev. D **66**, 076011 (2002), arXiv:hep-ph/0204226.
- [15] A. Ayala, P. Amore and A. Aranda, *Pion dispersion relation at finite density and temperature*, Phys. Rev. C **66**, 045205 (2002), arXiv:hep-ph/0207081.
- [16] R. D. Pisarski and M. Tytgat, *Propagation of cool pions*, Phys. Rev. D **54**, 2989 (1996), arXiv:hep-ph/9604404; *ibid.*, *Cool pions move at less than the speed of light*, in *Proceedings of the Con-*

- tinuous Advances in QCD, Minneapolis, MI*, 196, (1996), arXiv:hep-ph/9606459; *ibid. Scattering of soft, cool pions*, Phys. Rev. Lett. **78**, 3622 (1997), arXiv:hep-ph/9611206.
- [17] D. Toublan, *Pion dynamics at finite temperature*, Phys. Rev. D **56**, 5629 (1997), arXiv:hep-ph/9706273. U. G. Meissner, J. A. Oller and A. Wirzba, *In-medium chiral perturbation theory beyond the mean field approximation*, Annals Phys. **297** (2002) 27, arXiv:nucl-th/0109026.
- [18] N. Bilic and H. Nikolic, *Superluminal pions in a hadronic fluid*, Phys. Rev. D **68**, 085008 (2003), arXiv:hep-ph/0301275. J. Alexandre, J. Ellis and N. E. Mavromatos, *On the Possibility of Superluminal Neutrino Propagation*, Phys. Lett. B **706**, 456 (2012), arXiv:1109.6296 [hep-ph].
- [19] V. I. Ritus, *Radiative corrections in quantum electrodynamics with intense fields and their analytical properties*, Ann. Phys. **69**, (1972) 555.
- [20] K. Fukushima, D. E. Kharzeev and H. J. Warringa, *Electric-current susceptibility and the chiral magnetic effect*, Nucl. Phys. A **836**, 311 (2010), arXiv:0912.2961 [hep-ph].
- [21] N. Sadooghi and F. Taghinavaz, *Local electric current correlation function in an exponentially decaying magnetic field*, Phys. Rev. D **85**, 125035 (2012), arXiv:1203.5634 [hep-ph].
- [22] K. Heckmann, M. Buballa and J. Wambach, *Chiral restoration effects on the shear viscosity of a pion gas*, Prog. Part. Nucl. Phys. **67**, 348 (2012), arXiv:1202.0724 [hep-ph].
- [23] I. A. Shushpanov and A. V. Smilga, *Quark condensate in a magnetic field*, Phys. Lett. B **402**, 351 (1997), arXiv:hep-ph/9703201.
- [24] E. Quack, P. Zhuang, Y. Kalinovsky, S. P. Klevansky and J. Hufner, *π - π scattering lengths at finite temperature*, Phys. Lett. B **348**, 1 (1995), hep-ph/9410243.
- [25] G. S. Bali, F. Bruckmann, G. Endrodi, Z. Fodor, S. D. Katz, S. Krieg, A. Schafer and K. K. Szabo, *The QCD phase diagram for external magnetic fields*, JHEP **1202**, 044 (2012), arXiv:1111.4956 [hep-lat]; *ibid.* PoS LATTICE **2011**, 192 (2011), arXiv:1111.5155 [hep-lat]. G. S. Bali, F. Bruckmann, M. Constantinou, M. Costa, G. Endrodi, Z. Fodor, S. D. Katz, S. Krieg, H. Panagopoulos and A. Schafer, *Thermodynamic properties of QCD in external magnetic fields*, PoS ConfinementX, 198 (2012), arXiv:1301.5826 [hep-lat]. M. D'Elia, *Lattice QCD simulations in external background fields*, Lect. Notes Phys. **871**, 181 (2013), arXiv:1209.0374 [hep-lat].
- [26] E. S. Fraga and L. F. Palhares, *Deconfinement in the presence of a strong magnetic background: An exercise within the MIT bag model*, Phys. Rev. D **86**, 016008 (2012), arXiv:1201.5881 [hep-ph]. J. O. Andersen and A. A. Cruz, *Two-color QCD in a strong magnetic field: The role of the Polyakov loop*, Phys. Rev. D **88**, 025016 (2013), arXiv:1211.7293 [hep-ph]. F. Bruckmann, G. Endrodi and T. G. Kovacs, *Inverse magnetic catalysis and the Polyakov loop*, JHEP **1304**, 112 (2013), arXiv:1303.3972 [hep-lat]. N. Callebaut and D. Dudal, *On the transition temperature(s) of magnetized two-flavour holographic QCD*, Phys. Rev. D **87**, 106002 (2013), arXiv:1303.5674 [hep-th]. J. Chao, P. Chu and M. Huang, *Inverse magnetic catalysis induced by sphalerons*, arXiv:1305.1100 [hep-ph]. W. -C. Syu, D. -S. Lee and C. N. Leung, *External magnetic fields and the chiral phase transition in QED at nonzero chemical potential*, arXiv:1307.8222 [hep-ph].
- [27] K. Fukushima and Y. Hidaka, *Magnetic catalysis vs magnetic inhibition*, Phys. Rev. Lett. **110**, 031601 (2013), arXiv:1209.1319 [hep-ph].
- [28] F. Preis, A. Rebhan and A. Schmitt, *Inverse magnetic catalysis in dense holographic matter*, JHEP **1103**, 033 (2011), arXiv:1012.4785 [hep-th].
- [29] T. Inagaki, D. Kimura and T. Murata, *Four fermion interaction model in a constant magnetic field at finite temperature and chemical potential*, Prog. Theor. Phys. **111**, 371 (2004), hep-ph/0312005.
- [30] Sh. Fayazbakhsh and N. Sadooghi, *Phase diagram of hot magnetized two-flavor color superconducting quark matter*, Phys. Rev. D **83**, 025026 (2011), arXiv:1009.6125 [hep-ph].
- [31] M. Oertel, M. Buballa and J. Wambach, *Meson loop effects in the NJL model at zero and nonzero temperature*, Phys. Atom. Nucl. **64**, 698 (2001), [Yad. Fiz. **64**, 757 (2001)] arXiv:hep-ph/0008131.
- [32] J. O. Andersen, *Thermal pions in a magnetic background*, Phys. Rev. D **86**, 025020 (2012), arXiv:1202.2051 [hep-ph].
- [33] J. O. Andersen, *Chiral perturbation theory in a magnetic background - finite-temperature effects*, JHEP **1210**, 005 (2012), arXiv:1205.6978 [hep-ph].
- [34] V. Skokov, *Phase diagram in an external magnetic field beyond a mean-field approximation*, Phys. Rev. D **85**, 034026 (2012), arXiv:1112.5137 [hep-ph]. K. Fukushima and J. M. Pawłowski, *Magnetic catalysis in hot and dense quark matter and quantum fluctuations*, Phys. Rev. D **86**, 076013 (2012), arXiv:1203.4330 [hep-ph]. J. O. Andersen and A. Tranberg, *The Chiral transition in a magnetic background: Finite density effects and the functional renormalization group,* JHEP **1208**, 002 (2012), arXiv:1204.3360 [hep-ph].